



جامعة محمد بن راشد
للطب و العلوم الصحية

MOHAMMED BIN RASHID UNIVERSITY
OF MEDICINE AND HEALTH SCIENCES

EFFECT OF VOXEL SIZE ON THE ACCURACY OF AIRWAY VOLUMETRIC MEASUREMENTS USING CONE BEAM COMPUTED TOMOGRAPHY

Word Naeem Khaled Alhawi

BDS, University of Science and Technology, Sana'a, 2012

Submitted to the Hamdan Bin Mohammed College of Dental Medicine,
Mohammed Bin Rashid University of Medicine and Health Sciences
in Partial Fulfillment of the Requirements for the Degree of
Master of Science in Orthodontics

2021

ABSTRACT

Effect of Voxel Size on the Accuracy of Airway Volumetric Measurements Using Cone Beam Computed Tomography

Worod Naeem Khaled Alhawi, DDS

Principal Supervisor: Professor Ahmed Ghoneima

Co-supervisor: Dr. Samira Diar-Bakirly

AIM: The purpose of this retrospective study was to evaluate the accuracy and reliability of the airway volume, dental, and skeletal parameters measured digitally on cone beam computed tomography scans (CBCTs) using airway model scanned with different resolutions.

MATERIAL AND METHOD: This retrospective study was performed using CBCT images obtained from an artificial model of airway made by an acrylic airway model scanned at different voxel sizes, timing, and segmentation levels. CBCT scans were divided into four groups according to the voxel size of each scan (0.2, 0.25, 0.3 and 0.4). Airway volume parameters were measured using Dolphin 3D (Dolphin Imaging & Management solutions, Chatsworth, California, USA) software version 11.95. Reliability and accuracy were assessed by using intraclass correlation and Student's t-test. A P-value of less than 0.05 was considered significant.

RESULTS: The intra- and inter-examiner reliability were high for all measurements. Significant statistical differences were detected among airway volume measured at variable voxel size, scanning time, and segmentation level however, no significant differences were found in the skeletal and dental parameters. These results suggested that the airway measurements vary according to the voxel size, scanning time and segmentation level.

CONCLUSION: Airway volume measurements vary depending on the voxel size, scanning time and segmentation level of CBCT scans. Clinicians and researchers should be aware of the effect of the voxel size and scanning resolution on the airway measurements since this could affect the clinical judgement of critical cases.

DEDICATION

This study is dedicated:

To my uncle, Aiser Khaled Alhawi for his unconditional love and support during the past three years; without him I wouldn't have been able to pursue my dream.

To my loving mother, and siblings, for their continuous support.

To my friends, for their encouragement to finish this study.

To my professors, who planted the seeds of motivation and hard work.

And to my only source of enlightenment "God", thank you for giving me the strength and guidance to see this through.

DECLARATION

I hereby declare that the dissertation entitled “Effect of Voxel Size on the Accuracy of Airway Volumetric Measurements Using Cone Beam Computed Tomography” submitted by me for the partial fulfillment of the Master of Science in Orthodontics at the Hamdan Bin Mohamed College of Dental Medicine (HBMCDM), Mohammed Bin Rashid University of Medicine and Health Sciences (MBRU) is my original work under the direct supervision of Associate Professor Ahmed Ghoneima, and that the thesis has not previously formed the basis for the award to me of any degree, diploma, fellowship or any other title in this university or any other institution.

Name: Worod Naeem Alhawi

Signature:

ACKNOWLEDGMENT

First and foremost, I thank Allah who enabled me to finish my thesis. Then, I would like to submit my heartiest gratitude to my respected Professor A. Ghoneima, Doctor S. Diar-Bakirly and Professor Amar Hasan for their guidance and help to complete this project.

TABLE OF CONTENTS

ABSTRACT.....	Error! Bookmark not defined.
DEDICATION.....	Error! Bookmark not defined.i
DECLARATION.....	Error! Bookmark not defined.iv
ACKNOWLEDGMENTS	Error! Bookmark not defined.
TABLE OF CONTENTS	vii
LIST OF TABLES	Error! Bookmark not defined.
LIST OF FIGURES	ix
1. INTRODUCTION	
.....	Error! Bookmark not defined.
2. REVIEW OF THE LITERATURE	3
2.1 Airways Anatomy	3
2.1.1 Impact of different orthodontic treatment modalities on airway	5
2.1.2 Mouth breathing patient	11
2.1.3 Long face syndrome (adenoid patient)	16
2.2 Airway assessment for orthodontic patients	20
2.3 Imaging Tools	24
2.3.1 Lateral Cephalometry	24
2.3.2 CBCT	26
2.3.3 MRI	31
2.4 Accuracy and reliability of CBCT measurement	33
2.4.1 Accuracy of skeletal and dental measurements	34
2.4.2 Accuracy of soft tissue measurements	35
2.4.3 Accuracy of airway measurements	35
2.5 Effect of voxel size on airway measurements	36
3. AIM	40
4. MATERIALS AND METHODS	
.....	4Error! Bookmark not defined.
4.1 Statistical methods and reliability test	43
5. RESULTS	50

6. DISCUSSION60

7. CONCLUSIONS

.....Error! Bookmark not defined.**65**

8. REFERENCES

.....Error! Bookmark not defined.**66**

LIST OF TABLES

Table 1: The selected scanning settings used in the study	42
Table 2: Interrater reliability	52
Table 3: Comparison of airway volume measurements showing the effect of different scanning time (14.7 and 26.9 seconds) on the same voxel size	53
Table 4: Comparison of airway volume measurements showing the effect of different scanning time (4.7 and 8.9 seconds) on the same voxel size	54
Table 5: Comparison of skeletal and dental measurements showing the effect of different scanning time (14.7 and 26.9 seconds) on the same voxel size	54
Table 6: Comparison of skeletal and dental measurements showing the effect of different scanning time (4.7 and 8.9 seconds) on the same voxel size	55
Table 7: The effect of different voxel sizes (0.2 vox and 0.25 vox) on the airway volume measurements using the same scanning time	56
Table 8: The effect of different voxel sizes (0.3 vox and 0.4 vox) on the airway volume measurements using the same scanning time	57
Table 9: Comparison of Skeletal measurements for the time 14.7 sec and 26.9 sec between two different resolution (0.2vox & 0.25 vox)	57
Table 10: Comparison of Skeletal measurements for the time 4.7 sec & 8.9 sec between two different resolution (0.3vox & 0.4 vox)	58

Table 11: Comparison of airway volume measurements between different resolution regardless the time	59
Table 12: Comparison of Skeletal measurements between different resolution regardless the time	60

LIST OF FIGURES

Figure 1: The anatomical sections of the upper airway.....	5
Figure 2: The points and lines most commonly used to assess upper airway obstruction	24
Figure 3: The steps of making an artificial airway model.....	41
Figure 4: 3D CBCT skull volume A) right side, B) frontal view, and C) left side.....	44
Figure 5: 3D CBCT image orientation: frontal view	44
Figure 6: Image orientation: sagittal views	45
Figure 7: (A)sagittal section ,(B) sagittal section showing air way ,(C) 3D view showing airway volume	45
Figure 8: The airway boundaries traced on the midsagittal section.....	46
Figure 9: The Airway was segmented at different levels starting from S10 to S80 with increasing increment of S5 between each level.....	47
Figure 10: 3D image showing the airway volume.....	48
Figure 11: 3D image showing the A) the distance between the head of condyle to the coronoid process, and (B) the distance between the head of condyle to Goinion point..	48
Figure 12: CBCT sagittal section showing the A) maxillary length, and B) the lower anterior facial hight.....	49
Figure 13: 3D image showing A) the length and B) width of UR1.....	49

1. INTRODUCTION

Three-dimensional analysis of the airway volume has become of great interest to many clinicians because of the technological advances in imaging systems and software programs. The development of 3D imaging systems such as cone-beam computed tomography (CBCT) scanners, and medical imaging software is under continuous improvement which increased the ability to accurately evaluate the craniofacial structures and assess the airway volume in a more comprehensive way (Aboudara et al., 2009).

Accurate evaluation of the airway is an essential step to obtain proper diagnosis for patients with breathing disorders. Compared to normal subjects, obstructive sleep apnea (OSA) subjects may have substantial craniofacial differences in the size and position of the jaws or anomalies in the upper airway that might be associated with abnormalities in the size of the tongue and the soft palate. 3D imaging analysis of the airway has provided a reliable method that could be used as a useful tool for patient's diagnosis and treatment planning (Ogawa et al., 2007).

Several methods can be used to assess the airway structure for orthodontic patients such as nasal resistance pressure, acoustic rhinometry, nasopharyngolaryngoscopy, imaging tool which entails two-dimensional (2D) and 3D imaging modalities such as 2D lateral cephalograms, CBCT, and magnetic resonance imaging (MRI). Cone-beam computed tomography (CBCT) has been widely used in orthodontics since its introduction in dentistry in 1998. Researchers have assessed the accuracy and reliability of CBCT by scanning dry skulls or head phantoms to study the capability of CBCT in providing precise measurements of the craniofacial structures. Applications of CBCT images in orthodontics include dental measurements, evaluation of root resorption, evaluation of the temporomandibular joints, airway assessment, three-dimensional (3D) cephalometry, and

evaluation for orthognathic surgery (Isidor et al., 2018). This technology generate 3D images that are composed of voxels (Fokas et al., 2018).

A Voxel is the smallest distinguishable box-shaped unit of a 3-dimensional image, and determines the resolution of the images, and scan time, and affect the CBCT reconstruction time. Smaller voxels are associated with a higher resolution and subsequently greater radiation exposure. In CBCT imaging, voxels are isotropic and range from 0.4 mm³ to as small as 0.075 mm³. The use of smaller voxel sizes reduces the negative effects of partial-volume averaging, which occurs when the voxel size of the scan is greater than the size of the object to be imaged (Chen et al., 2018).

The purpose of this retrospective study was to evaluate the accuracy, reliability of the airway volume, dental, and skeletal parameters were measured digitally on CBCTs using airway model scanned with different resolution.

2. LITERATURE REVIEW

2.1. Airway anatomy

Breathing allows for a simple exchange of gases between venous blood and atmospheric air; the air gives part of its oxygen to the blood, and the blood releases carbon dioxide and water vapor into the air. Through the reciprocal effect of this gas exchange, venous blood recovers all its chemical and biological qualities, and becomes arterial blood (Downard et al., 2021).

The essential organs of the respiratory system are the lungs, located on either side of the thorax, on each side of the heart, and the great vessels. To reach the lungs, atmospheric air follows a long passage, the airway, which comprises the nasal cavity and incidentally the mouth. Then it includes successively the pharynx, larynx, trachea, and bronchi. The upper airway is formed by the nasal cavity and the pharynx (Kazemi et al.2018).

a) Nasal cavity

The airway starts, from the functional perspective, in the nostrils. The nasal airway includes the nose, the nasal cavities, and extend nasopharynx. In addition to breathing, the nose serves specific functions, such as smell and phonation (Rojas et al., 2017).

A deviated nasal septum, narrow nasal cavity, and turbinate hypertrophy are some of the that may cause mouth breathing and OSAS. In allergic rhinitis, which is also related to upper airway obstruction, the nasal mucous membrane swell with dust particles, pollen or even cold, also affecting the eyes and nose and causing a decrease in air flow (Park et al., 2017).

b) Pharynx

The pharynx is a tube-like structure formed by muscles and membranes. It measures approximately 12-14 cm and is divided into three parts: nasopharynx, oropharynx and laryngopharynx (Yin et al., 2018).

The nasopharynx is the upper part of the respiratory system. It is located behind the nasal cavity and on the soft palate. The nasopharynx is lined with a mucous membrane of respiratory epithelium, and becomes transitional epithelium in the oropharynx. In the roof submucosa there is a collection of lymphoid tissue called pharyngeal tonsil (adenoids), which, when large in size, is the main obstruction to the passage of air through the nasopharynx (Wally et al., 2020).

The oropharynx extends from the second to the fourth vertebra and opens into the oral cavity through an isthmus. The upper end is the soft palate, and the lower end is the lingual side of the epiglottis. The tongue is the main blocking element in the oropharynx, due to the general decrease in tone of the genioglossus muscle, which contracts to move the tongue forward during inspiration, and in this way, acts as a pharyngeal dilator (Metz, 2018).

The laryngopharynx joins the oropharynx at the pharyngoepiglottic fold and hyoid bone, and continues up to the sixth vertebra. It is behind the opening in the larynx. The outer wall is formed by the thyroid cartilage and the thyroid membrane (Pérez et al., 2017).

The airway, or respiratory tract, describes the organs of the respiratory tract that allow airflow during ventilation. They reach from the nares and buccal opening to the blind end of the alveolar sacs. They are subdivided into different regions with various organs and tissues to perform specific functions. The airway can be subdivided into the upper and lower airway, each of which has numerous subdivisions as follows (Jayashree, 2020).

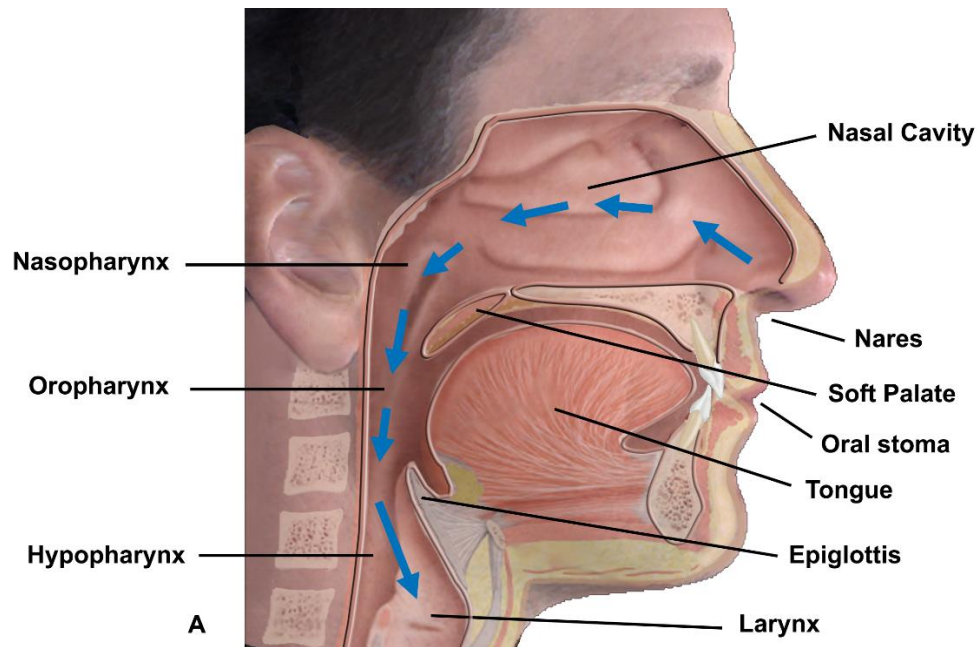


Fig. (1): The anatomical sections of the upper airway.

2.1.1 Impact of different orthodontic treatment modalities on Airway

The mutual interaction between the pharyngeal structures and the skeletal relationship is a subject of interest for the orthodontists and maxillofacial surgeon. Orthodontists believe that evaluation of soft tissues including facial contours, neuromuscular function, tongue, tonsil, adenoids and nasal polyps should be an integral part of orthodontic diagnosis and treatment planning. The pharyngeal airway is an intricate structure. In conjunction with its surrounding structures, it is responsible for the physiologic processes of swallowing, vocalization, and respiration (Maurya et al., 2019).

Mouth breathing influence the facial form, and is considered a predisposing factor to the development of the “long face syndrome” or “adenoid facies”. The characteristic of mouth breathing subject includes increased lower anterior facial height, retrognathic mandible, proclined maxillary incisors, high v-shaped palatal vault, maxillary constriction, flaccid and short upper lip, flaccid perioral musculature and dull appearance due to a constant open-mouth posture. Mouth

breathing was correlated with lowered position of the hyoid bone and anterior - inferior postured tongue with significant downward inclination of the mandible. On the other hand, the typical feature of the long face syndrome was the expression of a hereditary pattern (somatotype) and that mouth breathing was unrelated and should not be considered as an etiological factor and that could only be a para-phenomenon (Al-Qawasmi et al., 2020).

Obstructive sleep apnea (OSA) syndrome is characterized by temporary occlusion of the upper airway several times during the night which may result in hypoxia and sleep fragmentation and that the main symptoms were chronic tiredness, day-time somnolence associated with snoring and intellectual deterioration. A decrease in the upper airway dimension at the velopharyngeal level together with an increase in soft palate and tongue dimensions was observed. In the study (Balamurugan, 2019) it was found that the body mass index of patients was not related to positional changes of the hyoid bone. The airway impairment has also been associated with syndromes such as Apert's or Crouzon's. Both syndromes were characterized by severe maxillary hypoplasia, which has been suggested as the source of airway obstruction in the affected subjects (Balamurugan, 2019).

Studies on the changes of upper airway dimensions have consisted of analyzing the post-treatment effects of RME with dental casts, human skull models, 2-dimensional cephalometric radiographs, 3-dimensional imaging techniques including magnetic resonance images, Computed Tomography (CT), Cone-beam computed tomography (CBCT) systems, acoustic rhinometry and computed rhinomanometry (Manhar et al., 2019).

Among all the existing 3D imaging techniques, CBCT has become an alternative technique to conventional CT scanning for a comprehensive head and neck evaluation due to its significantly lower overall effective radiation dose and greater spatial resolution than medical CT, high contrast

between the hard and soft tissues, lower cost and easier access and availability to dentists. Despite the fact that with CBCT, it is not possible to discriminate between the various soft tissue structures, it is possible to determine the boundaries between soft tissues and air spaces making CBCT a potential diagnostic method to analyze airway dimensions (Stratis et al., 2017).

Impact of different orthodontic treatment modalities on airway

a) Surgical Treatment:

Several studies have reported that there was relative narrowing of the airway space after mandibular surgical set-back. Other studies have reported that the successful treatment of OSA was found to be associated with the mandibular surgical advancement. On the contrary, there were studies which found no difference in the airway size after surgical set back of the mandible. It has been reported that there was a lowering in the position of the hyoid bone over time in asymptomatic male controls and after mandibular set-back surgery. The finding suggested that it could be a physiologic phenomenon related to the increase of airway resistance or airway length. However, the position of the hyoid bone was moved in the opposite direction with mandibular advancement surgery. Lowe et al. mentioned that it is very important to observe the ratio between soft palate and pharyngeal space to preserve correct speech and prevent sleep apnea in later life. They focused on the treatment of skeletal Class III subjects involving maxillary protraction which was stated to disturb the afore-mentioned balance causing speech difficulty after therapy. In one of the study to evaluate the effect the maxillary advancement or impaction combined with maxillary setback on pharyngeal air way and maxillary sinus volume, it was reported that there was a significant decrease only for lower and total pharyngeal airway volumes in males and a significant decrease in the volume of the maxillary sinuses (AlKawari et al., 2018).

It was found that maxillomandibular advancement increased airway dimensions by increasing the distance from the occipital base to the pogonion. An increase of this distance showed a significant correlation with an improvement in the apnea-hypopnea index and a decreased pressure effort of the upper airway. Decreasing the pressure effort will decrease the breathing workload. This improves the condition of obstructive sleep apnea syndrome. The upper airway became wider in patients with Class II malocclusion deformity who had undergone mandibular advancement. However, this might become narrower with time (Xiang et al., 2017).

b) Orthopedic Treatment:

The sagittal dimension of the upper airway was significantly increased following functional appliance therapy in growing Class II patients. An increase in the superior upper-airway dimension by maxillary protraction was also observed. A possible explanation given was that, the maxillary forward growth could bring the tongue to a more anterior position causing the soft palate to come to a more anterior position; thus increasing the upper pharyngeal dimension. In a long term study it was found that the increase in the nasopharyngeal airway of patients with maxillary protraction continued to be significant even after a four-year follow up period while a significant increase in the oropharyngeal space was observed only after the follow-up period (Shuhart et al., 2019).

Rapid maxillary expansion (RME) is an orthodontic and orthopedic treatment option to correct posterior crossbites and maxillary transverse deficiencies. RME appliances produce heavy forces that result in skeletal or orthopedic expansion and also dentoalveolar changes. When the maxillary dental arch is rapidly expanded, the maxillary and palatine bones disarticulate along the midpalatal suture, and there are also changes to the frontomaxillary, zygomaticomaxillary, zygomaticotemporal, and pterygopalatine sutures. Stress distribution and displacement pattern

studies have evaluated the effects of RME on the craniofacial complex. A finite element analysis showed minimum displacement of the pterygoid plates near the cranial base and maximum displacement in the areas of the maxillary central incisors and the anteroinferior border of the nasal septum. A previous study also demonstrated that the lateral structures of the nasomaxillary complex moved upward, and midline structures, including ANS and A-point, moved downward. It was confirmed clinically that midpalatal sutural separation occurred in a triangular pattern with the wider base in the anterior part of the maxilla, and the effects of RME extended to the surrounding nasal and craniofacial structures (Smith et al., 2012).

RME is routinely used in the orthodontic treatment of patients with transverse maxillary deficiency, dental crowding, and/or a mandibular functional shift. A common form of RME uses tooth-borne expanders with bands on molars and sometimes first premolars. Transverse expansion is achieved through skeletal expansion, ie, opening of midpalatal sutures with separation of maxillary halves and dentoalveolar expansion, which can include buccal tipping of teeth and alveolar bending. Tooth-borne expansion appliances produce varying amounts of dental and skeletal expansion. Skeletal expansion is about half or less of the total amount of resulting expansion in adolescent patients. As the midpalatal sutures undergo maturation and fusion from childhood to late adolescence and adulthood, the amount of skeletal expansion with conventional RME and its long-term stability decreases. Failure of RME to open the suture is associated with unwanted dentoalveolar side effects, such as pain, severe buccal tipping and extrusion of teeth, gingival recession, buccal cortex fenestration, and root resorption (Kavand et al., 2019).

A mandibular advancement device in sleep apnea patients increased the pharyngeal airway and a reduction of the distance of the hyoid bone to the mandibular plane. The mechanism of action of the cervical headgear was associated with expansion and an upward and forward rotation of the

maxilla. This could be accompanied by an increase in the upper airway space and could be favorable for breathing. Maxillary expansion was shown to reduce upper airway obstruction during sleep in young adults with mild or moderate obstructive sleep apnea. RME produced a numerically parallel expansion of the mid palatal suture and a triangular shape of expansion with the base facing anteriorly when percentage change was calculated (Cao et al., 2017).

Bone-borne RME (or miniscrew assisted RME) was recently proposed to minimize the unwanted dentoalveolar effects of RME and produce greater skeletal changes. In the bone-borne RME, palatal miniscrews are used as anchorage to transfer the expansion force directly to the skeletal structures. In two groups of late adolescent patients, Lin et al. reported significantly greater skeletal expansion, less buccal tipping of first molars, and less buccal dehiscence following the bone-borne RME than expansion with tooth-borne RME using a hyrax appliance (Mutha, 2017).

In regard to the airway, a moderate increase of the cross-sectional area adjacent to the hard palate was observed. This cross-sectional area increase was highly dependent on the expansion between the 1st molars. The RME effect on the airway diminished as it moved further away from the mid palatal suture possibly due to the compensation generated by the surrounding soft tissues in a 3D frame. The treatment with the X-bow appliance in Class II patients resulted in favorable increase in the oropharyngeal airway dimensions and volume. In one study, it was found that (RME/FM) therapy did not affect at all the volume of maxillary sinuses and actually inhibited the normal expected increase of the volume of the pharynx when compared with a control group comprising normal individuals (Di Carlo et al., 2017).

The RME therapy improved the nasal airway ventilation and was detected by computational fluid dynamics. Changes noted in the oropharynx may be due to the lack of a standardized position of the head and tongue at the time of image acquisition (Kannan et al., 2017).

c) Fixed Appliance Therapy:

There was no study reported in the literature regarding the effect of fixed orthodontic treatment on the airway dimensions. The effect of extraction versus non-extraction treatment on oropharyngeal airway volume with the aid of CBCT showed no significant differences in the oropharyngeal airway volume. It was found that extraction of the first premolars for the treatment of bimaxillary protrusion did not affect upper airway dimensions despite the significant reduction in tongue length and arch dimensions. Large incisor retraction leads to narrowing of the upper airway in adult bimaxillary protrusion patients. The extraction of upper premolars rather than non-extraction in patients decreased the pharyngeal airway space with mandibular prognathism who planned to have bimaxillary surgery. The Forsus™ Fatigue Resistant Device (FRD) produced dento alveolar changes but did not have any significant influence on posterior airway in young adult patients (Mummolo et al., 2018).

2.1.2 Mouth breathing patients

Breathing is one of the most vital functions of the human body. Every breath we take can have a positive or negative impact on our bodies depending on how it is performed; and it has been well established that normal breathing should be achieved through the nose. However, it may be detoured to the oral cavity in the presence of an airway obstruction (Valcheva et al., 2018).

During normal breathing, the abdomen gently expands and contracts with each inhalation and exhalation. There is no effort involved, the breath is silent, regular, and most importantly, through the nose. Abnormal breathing or mouth breathing on the other hand; is often faster than normal, audible, punctuated by sighs, and involves visible movements of the upper chest. This type of breathing is normally only seen when a person is under stress, but for those who habitually breathe through their mouths, the negative side effects of stress and over-breathing become chronic. Habitual mouth breathing has serious implications on an individual's lifelong health, including the development of the facial structures. It is very important to know the benefits of nasal breathing over mouth breathing, and provides a self-help exercise to help decongest the nose (Recinto et al., 2017).

Habitual mouth breathing, conversely, involves an individual breathing in and out through the mouth for sustained periods of time, and at regular intervals during rest or sleep (Ballikaya et al., 2018). It is well documented that mouth breathing adults are more likely to experience sleep disordered breathing, fatigue, decreased productivity and poorer quality of life than those who nasal-breathe. In children, the harmful effects of mouth breathing are far greater, since it is during these formative years that breathing mode helps to shape the orofacial structures and airways. Children whose mouth breathing is left untreated for extended periods of time, can set the stage for lifelong respiratory problems and including, a less attractive face to name a few. As a result, malocclusions such as a skeletal Class II or Class III, along with a long lower face height (characterized as "long face syndrome"), and high palatal vaults may also be noted. These resultant craniofacial alterations associated with mouth breathing can significantly aggravate or increase the risk of snoring and obstructive sleep apnea in both children and adults (McKeown & Macaluso, 2017).

A study conducted demonstrated the critical role of the soft palate in determining oral or nasal airflow. The study showed that during mouth breathing, the soft palate will tend to move posteriorly against the posterior pharyngeal wall, thus closing the nasopharyngeal airway. Whereas, during nasal breathing, the soft palate moves inferiorly and anteriorly until it lays against the dorsum of the tongue, thus closing the oropharyngeal airway (Cappellette Jr et al., 2017).

The opening of the mouth during sleep in normal subjects and in patients with obstructive sleep apnea was also documented in this study. Mouth opening, even in the absence of oral airflow, has been shown to increase the propensity to upper airway collapse. The two most likely explanations for the latter finding are that jaw opening is associated with a posterior movement of the angle of the jaw and compromise of the oropharyngeal airway diameter, and that posterior and inferior movement of the mandible may shorten the upper airway dilator muscles located between the mandible and hyoid and compromise their contractile force by producing unfavorable length-tension relationships in these muscles. Therefore, it is of utmost importance to address mouth breathing accordingly (Kaur et al., 2018).

It has been noted that there is a lack of awareness regarding the negative impact of airway obstruction via mouth breathing on normal facial growth and physiologic health; and as a result, may be confused for (ADD) and hyperactivity. According to the National Sleep Foundation, attention deficit hyperactivity disorder (ADHD) is linked to a variety of sleep problems. Children and adults behave differently as a result of sleepiness. Adults usually become sluggish when tired while children tend to overcompensate and speed up. For this reason, sleep deprivation is sometimes confused with ADHD in children. Children may also be moody, emotionally explosive, and/or aggressive as a result of sleepiness. In a study involving 2,463 children aged 6-15, children

with sleep problems were more likely to be inattentive, hyperactive, impulsive, and display oppositional behaviors (Valcheva et al., 2018).

Another study published in the *International Journal of Pediatrics* investigating the long-term changes to facial structure caused by chronic mouth breathing noted that this seemingly ‘benign’ habit “has in fact immediate and/or latent cascading effects on multiple physiological and behavioral functions.” Therefore, with this in mind, mouth breathing can have a tremendous impact on the mental and physical health of children; as it can be associated with the restriction of the lower airways, poor quality of sleep, reduced cognitive functioning and a lower quality of life (Purwanegara, Sutrisna, 2018).

Brazilian researchers investigating the prevalence of mouth breathing in children ages three to nine found that a 55% random selection of 370 subjects were mouth-breathers. Reported causes of mouth breathing included: allergic rhinitis (81.4%), enlarged adenoids (79.2%), enlarged tonsils (12.6%), and obstructive deviation of the nasal septum (1.0%). The main clinical manifestations of mouth-breathers were: sleeping with the mouth open (86%), snoring (79%), itchy nose (77%), drooling on the pillow (62%), nocturnal sleep problems or agitated sleep (62%), nasal obstruction (49%), and irritability during the day (43%). ³ Although allergic rhinitis is considered one of the leading causes of respiratory obstruction; it is of utmost importance to note that upon the first onset of nasal congestion, a feeling of air deprivation occurs, causing the individual to switch to mouth breathing (McKeown, Macaluso, 2017).

Another study conducted demonstrated that orofacial changes were noted in mouth breathers such as: half-open lip and lower tongue position, lip, tongue and cheek hypo-tonicity, and tongue interposition between the arches during deglutition and phonation (Gutiérrez et al., 2021).

Effect of Low Tongue Position

A mouth breather carries the tongue in a low downward position, creating an airspace which allows the person to breathe more freely; and as a result it can lead to abnormal tongue activity. This abnormal tongue activity, can exert an excessive force upon the dentition during swallowing, contributing to malocclusions in children; and leading to periodontal disease and atypical myofascial pain in adulthood. This displacing force and misdirection of the tongue, can additionally contribute to microscopic changes in the attachment apparatus; leading to increased tooth mobility and advancing periodontal disease (Mozzanica et al., 2020).

Furthermore, this low tongue resting posture can contribute to various morphological changes to the orofacial structures; and consequently, Orofacial Myofunctional Disorders (OMDs) may develop as well. “OMDs are disorders pertaining to the face and mouth and may affect, directly and indirectly, chewing, swallowing, speech, occlusion, temporomandibular joint movement, oral hygiene, stability of orthodontic treatment, facial esthetics, and facial skeletal growth.” The most common forms of OMDs include: oral breathing or lack of habitual nasal breathing; habitual open mouth posture, and lack of lip seal with patent nasal passages; reduced upper lip movement with or without a restricted labial frenum; restricted lingual frenum, from borderline to ankyloglossia; anterior or lateral tongue thrust at rest (static posture); low and forward tongue position at rest, usually accompanied by an increased verticle dimension; inefficient chewing (related or not) to temporomandibular joint (TMJ) disorders or malocclusion; atypical swallowing, with or without a tongue thrust (dynamic posture); oral habits; and forward position of the head at rest, during chewing and during swallowing to name a few (Lun et al., 2019).

The resting posture of the tongue plays a pivotal role since its effects are far more constant than atypical swallowing. Mouth breathing encourages incorrect positioning of the tongue (on the floor

of the mouth), while nasal breathing naturally places the tongue in its proper resting position (on the roof of the mouth), and most important of all aides in achieving a lip seal (Grondin et al., 2017). A study conducted by (Purwanegara, Sutrisna, 2018) indicated that correct tongue resting position (on the roof of the mouth) resulted in a significant activity in the temporalis and suprahyoid muscles as well as a significant reduction in heart rate variability when compared with a low tongue resting position (on the floor of the mouth), In other words, a proper tongue resting posture is essential for achieving orofacial balance.

2.1.3 Long face syndrome (adenoid patients)

Long face morphology is a relatively common presentation among orthodontic patients. Classical features include an increased lower facial height, anterior open-bite and a narrow palate. While excessive vertical facial growth can often be recognized clinically, several cephalometric traits are commonly used to classify the underlying vertical skeletal pattern as normal (normodivergent), short (hypodivergent), or long (hyperdivergent). The term “long face syndrome” depicts only the vertical component of the three-dimensional problem which exists in these patients (Pawłowska-Seredyńska et al., 2020).

Both genetic and environmental factors have been associated with the etiology of excessive vertical facial development, although it is likely that more than one subtype of the phenotype exists. Etiological factors such as enlarged adenoids, nasal allergies, weak masticatory muscles, oral habits, and genetic factors have all been implicated in the development of the long face morphology. The treatment objective in a patient having sufficient potential for growth should be to restrain and control maxillary descent and prevent eruption of posterior teeth. When the severity of vertical deformity is so great that reasonable correction cannot be obtained by growth

modification or camouflage, the combination of orthodontics and orthognathic surgery may provide the only viable treatment. Despite being described extensively in the orthodontic literature the long face morphology still remains unclear. Most studies concentrate on only the open bite variant of this multifaceted problem. The aim of this article (Purwanegara, Sutrisna, 2018) is to comprehensively review the literature and present the varied clinical manifestations, etiology and available treatment modalities of the.

Two of the largest studies that investigated the prevalence of skeletal facial types were undertaken in the United States, and involved the evaluation of a large orthodontic based patient sample. In both studies, the prevalence of the long face pattern was approximately 22%. This extreme form of vertical craniofacial growth was also reported to be the second most common cause for seeking and receiving orthodontic/surgical treatment. The prevalence of these vertical growth patterns differed significantly according to Angle's classification of malocclusion, with the highest proportion occurring in the Class III sample (35%), followed by the Class I (32%), Class II Division 1 (30%) and Division 2 (18%) groups. These findings were consistent with those of another recent retrospective study investigating the occurrence of skeletal malocclusions in a Brazilian sample. Recently, Chew investigated the distribution of dentofacial deformities in an ethnically diverse Asian population receiving orthognathic surgery and found that the overall prevalence of vertical maxillary excess (VME) was nearly 22%, although significant differences existed in the distribution of VME among the three Angle classes. The highest prevalence of VME occurred in the Angle Class I (50%) and Class II malocclusions (48%), followed by the Class III group (10%) (Gupta et al., 2017).

Variations in the long face morphology have so far been discussed in terms of skeletal growth imbalances and mandibular rotations, although there still remains a great deal of uncertainty as to

what causes or “triggers” these growth patterns. The multiplicity of growth theories suggests a complex multi factorial etiology that involves genetic, environmental and epigenetic regulation. Several local environmental factors have been implicated in the etiology of the long face morphology; including nasal obstruction, para functional habits and weak muscle activity. Enlarged adenoids and a narrow nasopharynx are common causes of nasal obstruction that can prompt an individual to become a mouth breather. Theoretically, the downward and forward tongue position needed for oral respiration may also displace the mandible inferiorly and lead to an increase in vertical dimension. The long face morphology of mouth breathing children may also result from the effects of soft tissue stretching that commonly occur when these individuals overextend their heads to compensate for impaired nasal respiration. Several authors have found that long face individuals have a narrower nasopharynx than other facial types. In fact, both anterior and posterior facial heights appear to be positively correlated with all the volumetric measurements of the airway, with the exception of the middle pharyngeal third (Patel, 2019).

Oral habits such as digit sucking have been associated with the classical traits of the long face morphology. Non-nutritive sucking in the first few years of life is consistently associated with vertical malocclusions such as an anterior open bite. These non-nutritive sucking habits are often not limited to the vertical plane but may also affect the transverse dimension manifesting as posterior cross-bites. More recently, Thomas and colleagues used anthropometric points to describe facial morphology and found a high prevalence of severe facial convexity in adolescents who had been breastfed for relatively short periods and exhibited prolonged mouth-breathing habits that persisted until after the age of 6 years (Lorini et al., 2021).

Different heritability estimates have been reported for various vertical dimensions of the face. For instance, the heritability of total face height is reported to range from 0.8 to 1.3, while that of the

lower anterior face is between 0.9 and 1.6. In contrast, the heritability of the posterior and upper anterior face height ranges from 0.2 to 0.9 and 0.2 to 0.7, respectively. It is noteworthy, however, that heritability studies have a number of limitations that may account for some of the inconsistent findings reported in the literature. Since these estimates are typically derived under different environmental conditions, it is difficult to generalize the findings from one sample to another or even within the same sample over a substantial period of time (Saluja et al., 2020).

The long face morphology is typically associated with a number of classical features including a longer lower third of the face, facial retrognathism, depressed nasolabial areas, excessive exposure of the maxillary teeth and gingiva, lip incompetence, narrow palate, posterior cross-bites, and an anterior open-bite. Facial retrognathism, for example, gradually increases with facial divergence and mandibular plane angle. Other features (such as a dolichocephalic cranium, narrow nasal apertures, small temporal fossa, underdeveloped mandibular processes, narrow and long mandibular symphysis, reduced chin prominence, and large teeth) have also been reported in some individuals with the long face pattern (Purwanegara et al., 2017).

Anterior open bites are only found in a limited proportion of individuals with the long face morphology. Fields and colleagues recognized this common misconception and pointed out that “not all long faced patients have open-bites and not all open-bite patients are long faced”. The reduced prevalence of anterior open-bites in long face individuals can be attributed to the dentoalveolar compensatory mechanisms, which are capable of masking the underlying skeletal pattern in a large proportion of individuals (Aksoy et al., 2018).

2.2. Airway assessment for orthodontic patients

a) Acoustic rhinometry

It is the study of the geometry of the nasal cavity. It is based on the analysis of sound reflection and provides a calculation of cross-sectional areas of the nasal cavity and of certain nasal volumes. This is done by generating an audible sound in the nostril with an adapter, taking care not to deform the nasal vestibule. The sound wave penetrates the cavities and is reflected on the different nasal structures or their irregularities. Incident wave signals are measured and reflected according to time, which makes it possible to determine the distance, from the nostril, where there is a change in acoustic impedance. The most interesting data are the “minimum cross-sectional areas 1 and 2 (MCA1 and MCA2)”. MCA1 corresponds anatomically to the area at the nasal valve level (bounded by the caudal margin of the upper lateral cartilage and the nasal septum), which has the greatest resistance in the normal nose. MCA2 corresponds to the area at the level of the head of the inferior turbinate. As in active anterior RMM, the study can be performed before and after applying a vasoconstrictor for the same purpose and with a similar interpretation of the results (Miller et al., 2020).

b) Nasopharyngolaryngoscopy

This test evaluates the anatomy of the upper airway, as well as the soft palate, the movement of the vocal cords and the process of deglutition. It is performed with a flexible fiberscope which is inserted through the nasal cavities to observe both pharynx and larynx. The patient is usually awake, and topical lidocaine is applied on the nostrils and, as the case may be, vasoconstrictor (oxymetazoline). During the test, the patient may be asked to talk, cough or swallow, depending on what is being evaluated. The following anatomical elements should be evaluated: deviations of

the nasal septum, size of inferior turbinates, presence and size of the adenoid tissue, quantity and quality of nasal secretion, size of palatine tonsils and of the base of the tongue and its relationship with the oropharyngeal cavity, abduction of the vocal cords, subglottic diameter, and presence of masses or pathological deformities at any of these levels (Hernández, Clari, 2019).

c) Functional Nasal Permeability (PeNaF):

It is a clinical examination that assesses the independent functional nasal permeability of each cavity. The performance is recorded as negative (-) when the patient maintains nasal breathing for six inspirations at rest, and positive (+) when the patient fails to maintain it for six inspirations. A study validated in Chile recommends orthodontists implement this simple examination to rule out a possible nasal obstruction. If this is not the case, they should request an objective assessment to check the increase in nasal resistance (Rojas et al., 2017).

Upper airway assessment is essential in orthodontics because of the close interrelation between the correct respiratory function and the normal development of craniofacial structures (Li et al., 2020). The clinical examination, especially using Mallampatie's score, can give us an indication of the health of our patient's airway, which, together with the initial radiographic examination, shows us the need for further studies to rule out, for example, sleep disorders, which, with the right treatment, can restore our patients' health and greatly improve their quality of life (Wong, 2019). The cephalometric study of the nasopharynx is essential, as it can be easily assessed and it is a determining factor for the development of pediatric sleep disorders. The assessment of adenoid tissue with lateral cephalogram is a reproducible and easy-access exam in our daily work. However, it will never yield an accurate diagnosis of the airway volume, but rather it will indicate the need for a referral to an ENT specialist so that more comprehensive tests are run (Davis, 2020).

D) Nasal resistance pressure

Nasal resistance can be calculated on the basis of the pressure gradients formed in the nose during inspiration. Rhinomanometry (RM) measures nasal airway resistance and airflow. It has two phases, passive and active, and it can be divided into anterior and posterior. Active RM requires the patient to generate airflow through inspiration. Passive RM utilizes external generation of airflow through the nose at a constant pressure. Anterior RM may reflect the status of the nares, nasal valves, and nasal cycling, and utilizes a device inserted into the nares. Posterior RM, in turn, utilizes a sensor inserted into the mouth which measures the nasopharynx, hence requiring substantial patient co-operation. These tests are also usually performed before and after the administration of nasal decongestants (Cilluffo et al., 2020).

Acoustic rhinometry evaluates nasal obstruction by analyzing reflected sound waves introduced through the nares. It is not invasive, is easily reproducible and it does not require patient co-operation. The results are expressed as cross-sectional dimensions of the nasal cavity, which closely approximate the smallest cross-sectional area and volume (van Egmond et al., 2017).

The cross-sectional area (CSA) is measured at different points from the nares to the closest area of narrowing, which corresponds to the nasal valve area. Since a 'normal' CSA varies so much from patient to patient, an absolute value is not very useful for diagnosis or for confirmation of nasal valve area obstruction. Previously published work by the authors, however, has demonstrated that the ratio of the CSA during inspiration to the CSA at rest is highly diagnostic of nasal valve collapse. Normally, deep inspiration should not decrease the CSA. If it does, it is a sign of nasal valve collapse (Adarsh et al., 2018).

E) Rhinomanometry

It aims to objectively evaluate nasal obstruction. There are different types of rhinomanometry (RMM), active anterior RMM being the one most frequently used. This evaluates nasal airflow in inspiration and expiration by detecting potential obstructions and/or resistance. This can be done with a face mask or by placing an olive in each nostril; the first device has the advantage of not deforming the nostrils, reducing the possibility of leakage. However, it requires full patient cooperation and cannot be implemented if there is total occlusion of one nostril or a septal perforation (García-Sanz et al., 2017).

After placing the mask, airflows are measured with the rhinomanometer, and the data are analyzed computationally and then graphs are designed in pressure/volume curves. After a first measurement in basal conditions, the recording is repeated under the effect of a topical vasoconstrictor, which will differentiate mechanical obstructions (which do not vary with the vasoconstrictor), vasomotor obstructions (which fully improve with the vasoconstrictor) and mixed obstructions (which improve partially with the vasoconstrictor). In general, any cause of obstruction with bone, cartilage, or tissues, with little edema or whose vasoconstriction cannot be affected, as well as inflammatory etiologies, with edema and tissue susceptible to vasoconstriction, will yield vasomotor curves. The pathology which best represents mechanical obstruction is the deviated septum, and the main vasomotor obstruction is inferior turbinate hypertrophy (Van Dessel et al., 2017).

2.3. Imaging tools

2.3.1 Lateral cephalometry

Lateral cephalometry is commonly used in clinical practice given its relative simplicity, accessibility, low cost and low exposure to radiation (Friedrich et al., 2017). Cephalometric tracing can identify different characteristics that may indicate a narrow upper airway. Lateral cephalograms provide reliable linear measurements, can measure the dimensions of the nasopharyngeal and retropalatal regions, but have not proven to be reliable to measure the airway in the back of the tongue. However, this is a highly reproducible test using the natural position of the patient's head, provided that it is run correctly. A 2013 meta-analysis on craniofacial morphology found a significant relationship between a reduced upper airway at the pharynx level (mainly adenoid hypertrophy) and pediatric sleep disorders (David et al., 2017).

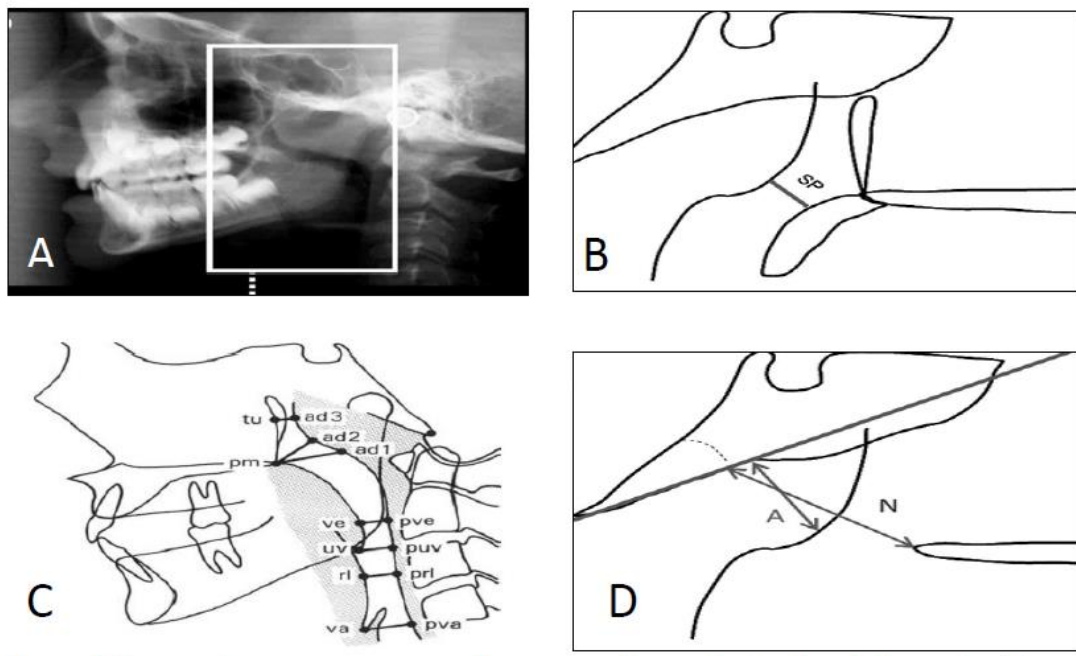


Fig. (2): The points and lines most commonly used to assess upper airway obstruction (da Costa et al., 2017).

McNamara, 1984 in his study stated that there is obstruction of the airway if there is a distance lower than 5 mm between the nearest points of the posterior wall of the nasopharynx and of the soft palate. In 1979, Fujioka et al. described the adenoidal-nasopharyngeal ratio (AN ratio), which relates the length of the line perpendicular to the sphenoid bone (A) by the thickest portion of the adenoids with the distance between the posterior nasal spine and the anterior edge of the sphenobasioccipital synchondrosis (N). An $AN < 0.8$ is considered normal and an $AN > 0.8$ is considered enlarged. In addition, another study in 2012 found that both parameters had good reproducibility and a variability which was not clinically significant (Kumar et al., 2019).

One of the most common reasons for upper airway obstruction is hypertrophic adenoids, defined as a collection of lymphoid tissues in the posterior wall of the nasopharynx which increase in volume as the immune activity increases. Before planning an orthodontic treatment, this area is usually observed in the lateral cephalometry, therefore, lateral cephalometry is used as a and reproducible diagnostic method which is easy to interpret when assessing the size of the adenoids. With the advent of CBCT, 3D images available to orthodontists. Studies have tried to correlate lateral cephalograms and CBCT relation to the linear volumes of the airway, but no clear consensus has been established (Chan et al., 2020). Adenoids develop progressively, with their highest growth achieved between 4 and 5 years of age, followed by another peak between 9 and 10, and then the size decreases progressively until 14 to 15 years of age (Spin-Neto et al., 2013).

A study was conducted to assess whether adenoidal ratio on lateral cephalograms can be used to estimate airway volumes, using CBCT as the validation method. They concluded that the lateral cephalogram can provide some information about the nasopharyngeal space, particularly in patients over 15. This is due to the stability reached by the tissue at this age; however, it cannot be used as a diagnostic procedure to determine the volume of the total airway, but rather as an

assessment tool to determine the need for a more comprehensive ENT examination. Fiber endoscopy is the most successful diagnostic test for adenoid hypertrophy. Of the radiological examinations, only cephalometry has proven useful for the study of the facial skeleton (Ghoneima, Kula, 2013).

2.3.2 CBCT

Cone beam computed tomography (CBCT) is a relatively new imaging technology that provides multi-planar images in submillimeter resolution. In the last years, CBCT has achieved wide acceptance in dentomaxillofacial imaging and has fundamentally replaced conventional tomography for several diagnostic tasks in dentistry. The main advantage of CBCT is its shorter acquisition time and patient radiation dose when compared to conventional CT (Chan et al., 2020). Since its development in 1990, the CBCT has been well adopted for diagnosis in the maxillofacial area, as it provides a 3D representation of the structures at a low cost and with an effective radiation dose which is much lower when compared to computed tomography (CT). Although CBCT is less effective than CT in tissue discrimination, it defines the boundaries between tissues and empty spaces with high spatial resolution. In addition, several studies have shown that it is accurate and reliable for upper airway assessment (Banerjee et al., 2020).

A single 360° rotational scan provides CBCT image data in a digital format. For image reconstruction, the obtained information is rendered into a 3-dimensional (3-D) image using an algorithm for volumetric tomography. These 3-D images made by CBCT are composed of voxel, which is the smallest image unit and determines image resolution. The size of each voxel is determined by its height, width and thickness and the spatial resolution of CBCT depends upon the voxel dimension. The smaller voxel dimension results in the greater image resolution; however,

higher radiation doses are needed for smaller voxel. In addition to the voxel size of the CBCT scanner, several other factors including the properties of the bone itself, the skill of the examiner (the person making the measurements), the software used to view and measure the CBCT images and the presence or absence of soft tissue at and around the area of interest may also potentially affect the accuracy of linear measurements of alveolar bone from CBCT images (Hekmatian et al., 2014).

Volumetric reconstructions that may be obtained from CBCTs help clinicians make a correct diagnosis and indicate a better treatment plan for some pathologies of the maxillofacial area, especially those related to the airway. Three-dimensional images and volumes can be obtained from two-dimensional slices with CBCT after a complex process, which involves the use of especially designed computer programs. For the volumetric reconstruction and visualization of the upper airway, these software programs must allow us to find the correct location of the boundaries of the pharynx and nasal cavity (segmentation) through a process that can be manual, automatic or semi-automatic. Three commercial software programs for the study of the airway were analyzed. They were found to have reliable reproducible and accurate results of linear measurements, but they lost accuracy when calculating the volume of the airway. This could be due to the automatic segmentation of the nasal cavity, the nasopharynx and oropharynx. Another study had the same results when analyzing six commercial software programs (Belgin et al., 2019).

Besides the differences found in the use of different programs, when assessing the volume of the upper airway we should consider the differences in the anatomical boundaries of the nasopharynx and oropharynx, reported in different studies. The upper boundary of the nasopharynx and the lower boundary of the oropharynx have the greatest variability, followed by the boundary between

these two structures. The oral cavity and the nasal cavity do not show variability in their boundaries (Alsufyani et al., 2017).

In clinical practice, the image quality of CBCT scans and the ability of CBCT to display anatomic features and pathology is influenced by a number of variables such as the scanning unit, the field of view (FOV), examined object, examination time, tube voltage and amperage, and also spatial resolution defined by the voxel size. The size of a voxel is defined by its height, width, and depth, and CBCT voxels are generally isotropic (the three parameters are equal). The voxel size of a 3D image is equivalent to the pixel resolution in 2D images, and, in this case, a resolution of 300 ppi (pixels per inch) would directly correlate to a voxel size of 0.085 mm. Images acquired in smaller voxel sizes, although “prettier” and sharper from a subjective point of view, will increase the radiation dose to the patient but might provide the same diagnostic outcome as lower resolution images. Thus, it is important to ponder that the comparison of CBCT examinations with various voxel settings is relevant to understand the impact of the inherent image quality on the reliability and accuracy of the diagnostic outcome (Yeh, Chen, 2018).

Airway volume and respiratory function are highly relevant to the orthodontic specialty. Studies have confirmed that airway problems are significantly related to different types of malocclusion and that nasal obstruction is a major etiological factor for dentofacial anomalies. For example, in growing patients with skeletal discrepancies and signs of adenoid facies, early diagnosis, prediction, and assessment of the functional etiological factors are critical for the restoration of normal craniofacial growth and the stability of the treatment outcome. Evaluation of the airway is an essential diagnostic step for patients with breathing disorders. Compared to normal subjects, obstructive sleep apnea (OSA) subjects have considerable craniofacial differences, such as the size and position of the mandible, enlargement of the posterior airway space, and size of the tongue

and the soft palate. In these patients, airway assessment has been mostly performed on two-dimensional lateral cephalograms by identifying special landmarks and measuring various lengths and areas in the airway region (McGuigan et al., 2018).

Most of the airway studies relating airway anatomy and the craniofacial growth and development are limited because of using the two-dimensional lateral or frontal cephalograms which cannot identify the soft tissue contour in the third dimension thus limiting evaluation of areas and volumes. Currently, the advances in computed tomography (CT) imaging and the three-dimensional technology allow better visualization of the airway and volumetric analysis. Clinicians can more easily perform the volumetric measurements and also calculate the cross-sectional areas of the airway in three planes of space: coronal, sagittal, and axial. The axial plane, which is not visualized on a lateral cephalogram, is the most physiologically relevant plane because it is perpendicular to the airflow. CBCT systems have been developed specifically for the maxillofacial region with the advantage of the reduced radiation doses compared with conventional CT. Accurate and easy evaluation of the airway anatomy has been possible using those CBCT systems. Although numerous studies have been published using CBCT to evaluate airway, few have addressed the accuracy of the measures. The aim of the study (De Felice et al., 2019) was to evaluate the accuracy and reliability of the airway volume measured digitally on CBCTs as well as the most constricted area in the airway compared to the manual measurements made on an airway model.

Alsufyani et al., in their 2012 review, suggest that the protocol proposed by EI and Palomo in 2010 should be replicated in other studies. The nasopharynx, on the sagittal plane, was delimited from the last slice before the nasal septum joins the posterior wall of the pharynx, on the sagittal plane; the lower boundary was determined by the palatal plane. The upper boundary of the oropharynx is the nasopharynx, and the lower one is the parallel to the plane that goes through the lowest

anterior point of the second cervical vertebra. These authors suggest using as lower boundary the section between the oropharynx to C2, and not a lower sector, such as C3, C4, or the epiglottis, because in this way we can use smaller windows and reduce the radiation dose patients receive. The segmentation was performed manually and 30-cm windows (FOV) were used, though a 13-cm window is acceptable to display the oropharynx or the nasopharynx and the nasal cavity (Lee et al., 2020).

We must also consider the head position and the position of the patient when the CBCT is taken to obtain accurate and repeatable upper airway measurements and volumes. The position of the hyoid bone and tongue, and the dimension of the airway would be highly reproducible using the natural position of the head when taking lateral cephalograms. In addition, it has been found that individuals would be approximately 40% more affected by the width of the airway in an upright position. Solow et al. determined that in an upright position or by increasing the cervical skull angle, there is an increase in upper airway diameters. Alsufyani states that images must be obtained with the patient in a sitting position so as not to affect airway diameter (Bates et al., 2019).

Two systematic literature reviews concluded that although major progress has been made in the capture and management of CBCT images, there is no optimized evidence-based protocol to obtain images to analyze the upper airway. Several obstacles must still be overcome, such as the influence of the position of the tongue, mandible morphology, the impact of the respiratory phase and the definition of the anatomical boundaries of the upper airway, as well as the lack of consistency in the configuration of the equipment and in how images and volumetric reconstructions are obtained (Elders et al., 2021). McCrillis et al., in a 2009 review, indicate a lack of studies to map the characteristics shown in the upper airway CBCT with clinical results according to the treatment modality, so that the various modalities are based on predictable outcomes (Chan et al., 2019).

CBCT is becoming commonplace in dental practice. It provides 3D images and axial slices of the airway at low cost and with an acceptable radiation dose for a specific image quality. However, there are still difficulties to overcome to be able to extrapolate the results of the scientific evidence on the upper airway to our population, given the large number of factors that have not been properly protocolized. Additionally, CBCT is not essential for airway diagnosis, as its volumetric calculations are static and change significantly depending on patient position, respiratory phase, etc. Hence the importance of the medical history, and of tools such as the sleep questionnaire, both for pediatric and adult patients, and not just the subjective evaluation of a diagnostic image (Yu et al., 2020).

2.3.3 MRI

Other image modalities may be valid for assessing different structures present in the craniofacial complex such as cartilage. Magnetic resonance (MRI) is often used for this purpose (Shaheen et al., 2017). MRI does not find widespread use for the purpose of planning airway management. This is because it is a costly, time-consuming diagnostic modality and requires sedation or general anaesthesia in paediatric and claustrophobic adult population, which itself requires proper airway control. Scanning of airway structures is compromised in MRI due to breathing motion artefacts and limited resolution. Also, unlike CT scan, the images cannot be reconstructed to form 3D image for better understanding of the patient's airway anatomy. As CT is good for diagnosing bony pathologies, MRI is superior in defining soft-tissue lesions and cartilage invasions, that too without the fear of radiation exposure. It is also better than CT for differentiating tumours from inflammatory states, which finds implications in oncoanaesthesia in patients treated with radiation

and chemotherapy. In spite of all this, MRI has some documented uses in airway evaluation (Jain et al., 2019).

A previous study compared several measurements using neck radiograph and MRI between unexpected DI and similar controls. They concluded that they could not validate any parameter sufficient enough to predict DI. Also, they did not find statistically significant difference among the values measured using both modalities. Elongated epiglottis (≥ 41 mm) and its abnormal angulation on MRI have been found to contribute to DA (Han et al., 2018).

MRI has also been used for finding appropriate size of endotracheal tube. Patients suffering from head and neck, thyroid, oesophageal or mediastinal cancers undergo MRI for tumour staging and for surgical planning. This scan can be used to formulate airway plan as well. Invasion of preepiglottic and paraglottic space should alert the anaesthesiologist because clinical examination in these cases may not hint at DA. Tracheobronchial invasion or compression by thyroid, oesophageal or mediastinal masses may be detected by MRI scan and hence aid in airway planning (Banko et al., 2014).

Dynamic MR studies may help in identification of uncommon causes of stridor, for example, hypermobile epiglottis, which may also hinder airway management (Breyer et al., 2009). Thus, even though MRI is not the preferred modality for pure airway evaluation, it can be easily used for understanding the pathophysiology of a patient's airway, especially if it has been done for aiding treatment, like in cases of cervical spine surgeries where it is usually done for formulation of surgical plan. This requires effective communication between the treating doctor, radiologist and the anaesthesiologist (Han et al., 2015).

2.4. Accuracy and reliability of CBCT measurements

Cone-Beam Computed Tomography (CBCT) has been proved to be an accurate and reliable method for measuring craniofacial structures. Several published studies have assessed its accuracy and reliability by scanning dry skulls in order to compare linear and volumetric measurements taken from physical structures and from CBCT images (Fokas et al., 2018). A previous study demonstrated the accuracy of CBCT for measuring volumes. Both studies applied Cavalieri's principle to CBCT images and compared the results with physical volume calculations based on the Archimedean principle (Pan et al., 2020).

Several studies conducted to evaluate the accuracy of CBCT have focused on the maxillary bones, while others have specifically studied the mandibular condyles, performing the CBCT scans on dry human skulls. However, such studies provide limited information because the soft tissue component is not considered. When soft tissues are present, their attenuation coefficients can decrease the quality of the image, and so the absence of these tissues, replacing them with air, increases contrast and accuracy (San José et al., 2017).

A previous study evaluated the accuracy of CBCT on linear measurements with the soft tissue intact. They used six embalmed heads, which were sectioned to introduce radiopaque markers before taking the CBCT scan. The structures were not extracted to perform the physical measurements, being directly measured on the section with intact soft tissues. No other studies have assessed the accuracy of CBCT on linear measurements with the soft tissues present when the CBCT scan was taken. Furthermore, to date, no investigation has analyzed the accuracy of CBCT for volumetric measurement in this context (Liao, Lo, 2018).

2.4.1 Accuracy of skeletal and dental measurements

Craniometric measurements have been used to aid orthodontic diagnosis over the past century. Direct craniometric and anthropometric measurements were used before the discovery of the x-ray and the introduction of the cephalometric method. The cephalostat, a modified version of the craniostat used for measuring skulls, was introduced by Broadbent in 1931.¹ Since then, cephalometry has become a commonly used diagnostic tool in orthodontics. Many studies have looked at the reliability of lateral cephalograms and have found them to be reproducible. Few studies, however, have attempted to assess the accuracy of cephalometric measurements as applied three-dimensionally because of known intrinsic limitations of these images, such as distortion and magnification (Zorba et al., 2018).

CBCT application as a craniofacial diagnostic tool often has been underutilized, with the orthodontist gathering 3D data and then synthesizing conventional two-dimensional (2D) films with which he or she is more familiar (eg, lateral headfilms, panoramic radiographs). These reconstructed images are accurate and reliable when compared with conventional radiographs and simulate the way lateral cephalometric or panoramic films are magnified and distorted. This so-called “bridge” from 3D to 2D images has helped orthodontists use the advantages of CT scans without having to add a lateral cephalometric exposure for craniofacial diagnosis (Barbic et al., 2017).

Today, existing software allows us to take full advantage of CT scans in performing 3D measurements and developing 3D craniofacial analyses. These 3D measurements, made on CT images, can be more accurate and reproducible and have the potential to aid in the craniofacial diagnosis of facial asymmetries, functional shifts, and canted occlusal planes (Richmond, 2018).

2.4.2 Accuracy of soft tissue measurements

Facial reconstruction is of great concern to the fields of forensic science and anthropology. Forensic facial reconstruction is a mixture of science and art in which the reconstruction of faces on skulls is attempted for the purpose of individual identification. Facial reconstruction is a method used in forensic anthropology to aid in the identification of skeletal remains and is dependent on the estimated soft tissue thickness over various anatomical sites of the cranial and facial regions (Jullabussapa et al., 2020).

There are two basic methods of modeling the face in forensic and anthropologic studies. One is a morphoscopic method using an anatomical approach for reconstructing the musculature, fat and skin. The other is a morphometric method using the average facial soft tissue thicknesses that have been gathered by previous researchers over various anatomical sites of the skull and jaws (Amaral et al., 2017).

Traditionally facial soft tissue measurements were studied using the needle depth probing method on cadavers. However, the accuracy of these measurements is questionable because of inaccurate orientation of the probe, perpendicular to the underlying bone, and compression caused by placing of the probe. As well, there is the difficulty in obtaining a large number of specimens representing a specific population, or ethnic or racial group, and the time consuming nature of such a study (Chen et al., 2017).

Several imaging-based methods for measuring living facial soft tissue thickness have been reported. These include lateral cephalometric radiography , computed tomography (CT) , ultrasound and magnetic resonance imaging. However, no study of the accuracy and reliability of these imaging modalities for measuring facial soft tissue thickness has been reported. Moreover,

there is no study of the effect of the changes in computed tomography scanning protocols (Chen et al., 2018).

2.4.3 Accuracy of airway measurements

The upper airway is an important and complex anatomical structure in respiratory medicine. The anatomical and functional abnormalities of the upper airway play an important role in the pathogenesis of many breathing disorders such as obstructive sleep apnea (OSA) (Tanabe et al., 2018).

Recently, CBCT has been used to analyze the upper airway three dimensionally. In this context, it is important to emphasize that the ever-increasing use of medical CT technologies since the 1980s has raised concerns about possible cancer risks. The radiation dose incurred by CBCT scanners is lower than that from medical CT scanners, which makes CBCT easier to justify as part of the diagnostic procedure (Quan et al., 2019).

After image acquisition, CBCT data sets are usually saved as digital imaging and communications in medicine files and imported into dedicated software packages for upper airway analysis. A wide variety of engineering, medical and dental software packages are currently available on the market. To the best of our knowledge, the reliability and accuracy of most software packages for upper airway analysis have not yet been tested (Lee et al., 2019).

One previous study concluded that several software packages showed high reliability in the volume measurement of the upper airway but without mentioning their reliability in the area of and linear measurements of the upper airway. Moreover, the study did not assess the accuracy of the upper airway measurements. Three previous studies have, however, used artificial phantom models of the upper airway as a gold standard to assess the accuracy of software packages. In this context, it

should be noted that such phantom models were mostly manufactured using generic forms, which do not correctly mimic the complex anatomy of the upper airway. Recent developments in the field of three-dimensional (3D) printing offer new opportunities for manufacturing life-like anthropomorphic phantoms. In the present study, an anthropomorphic phantom was manufactured based on the anatomical characteristics of a human. This is, to the best of our knowledge, the first time a humanoid phantom has been used to assess the accuracy of different imaging software packages for upper airway analysis (Ashmawy et al., 2017).

2.5. Effect of voxel size on airway measurements

Cone-beam computed tomography (CBCT) has been widely used in orthodontics since its introduction in dentistry in 1998. Applications of CBCT images in orthodontics include dental measurements, evaluation of root resorption, diagnoses of the temporomandibular joint, airway assessment, three-dimensional (3D) cephalometry, and evaluation of orthognathic surgery (Isidor et al., 2018).

The image quality of CBCT scan might be influenced by a number of variables, such as the scanning unit, the field of view (FOV), subject characteristics, scanning time, tube voltage and tube current, and also spatial resolution defined by the voxel size. CBCT volumetric data set is composed of volume elements called voxels and the dimension of each voxel determines spatial resolution of the image. Images acquired in smaller voxel sizes or smaller FOV have better spatial resolution. Maret et al. assessed the effect of voxel size on the accuracy of 3D reconstruction of CBCT data. They found that volumetric measurements at voxel size of 200 μ m and 300 μ m were underestimated by comparing with those obtained with voxel size of 76 μ m and 41 μ m. In

contrast, Damstra et al. suggested that there was no statistically significant difference of the linear measurement accuracy between 0.40 mm and 0.25 mm voxel size group (Eliliwi et al., 2020).

Landmark-based analysis of maxillofacial structure with linear and angular measurements is the most common method of cephalometric analysis in orthodontics since Broadbent introduced cephalometric radiography. However, in the literature, few studies so far have assessed the effect of voxel size on the accuracy of landmark identification in the CBCT images. The purpose of the present study was to investigate the effect of voxel size on the accuracy of landmark identification in CBCT images (Yilmaz et al., 2019).

Voxel size is of paramount importance in terms of quality and scanning and reconstruction times of CBCT images. A “voxel” describes the smallest distinguishable box-shaped part of a 3-dimensional image. In CBCT imaging, voxels are isotropic and range from 0.4 mm to as small as 0.075 mm. This superior spatial resolution, that is, the ability to discriminate objects of different attenuation separated by very small distances, is one of the most attractive qualities of CBCT imaging and is largely the result of flat panel technology and isotropic data acquisition. The use of smaller voxel sizes also reduces the negative effects of partial-volume averaging, which occurs when the voxel size of the scan is greater than the size of the object to be imaged. In such cases, the pixel is not representative of either the tissue or the boundary but is given a weighted average of the different CT values (Chen et al., 2018).

In general, radiation time and dose increase with smaller voxel sizes in order to decrease the noise that occurs when using smaller voxels. Thus, selection of voxel size can be critical in the diagnosis of various craniofacial structures when using CBCT (Dublin et al., 2017).

In 1997, Arai et al. developed cone-beam computed tomography (CBCT) for the diagnosis of impacted teeth, apical lesions, periodontitis, root fractures, enostosis, and temporomandibular joint

disease. The imaging area was originally 4 cm in diameter by 3 cm in height, and their machine was characterized by a high resolution and low-radiation dose. The voxel size was 0.125 mm isotropic because the image area was small. Images with this system could discern the periodontal ligament space very clearly, and the small radiation field of this machine resulted in a low exposure compared to other CBCT machines (Hayashi et al., 2018).

Subsequently, recent generations of CBCT were developed, most of which could image large areas of the maxilla and mandible, decreasing the noise, voxel size, or slice thickness while the other factors remained constant resulted in an increased radiation dose. In these CBCT systems, the voxel sizes used were 0.2–0.4 mm because of computational limitations. If the imaging area measured 8 cm in diameter by 8 cm in height, and a voxel size of 0.125 mm was applied, one would have 640 × 640 × 640 voxels. Similarly, for a voxel size of 0.080 mm, 1,000 × 1,000 × 1,000 voxels would be obtained, which made reconstruction difficult using personal computers (Zhao et al., 2020).

To solve this problem, the newest Accuitomo F8 (J. Morita, Kyoto, Japan) was developed with a maximum field of view (FOV) of 8 × 8 cm and a zoom reconstruction function. When the raw data are reconstructed, the function decreases the voxel size (zoom), which enlarges the image. To use this function, the region of interest (ROI) on the image is first chosen and then the region is reconstructed with a smaller voxel size (Shafiq-ul-Hassan et al., 2017).

3. AIM

The purpose of this retrospective study was to evaluate the accuracy and reliability of the airway volume, dental, and skeletal parameters measured digitally on cone beam computed tomography scans (CBCTs) using airway model scanned with different resolutions and scanning time.

4. MATERIALS AND METHODS

This retrospective study was performed using CBCT images obtained from an artificial model of airway. In order to create this artificial model, a wax model was first carved in a shape that matches the human airway passage in anatomy and size. A silicone impression was then taken and poured with plaster of Paris to convert the wax model into a stone model. The stone airway model was then adjusted on the platform of Biostar pressure molding machine (Great Lakes Orthodontics, Tonawanda, New York, USA) and covered with a transparent acrylic sheet. After the acrylic was hardened, the stone model was removed from inside and a transparent air-filled acrylic airway model was created Figure 3.

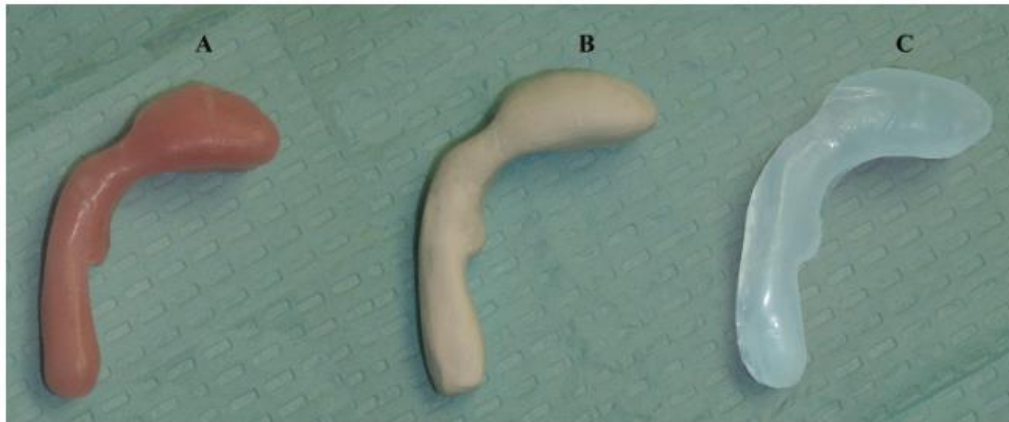


Figure 3: The steps of making an artificial airway model: (A) wax model, (B) stone model (C) air-filled acrylic model simulating the airway passage in shape and size.

The model was then attached to a human dry skull to simulate the normal position of the airway with overlapping hard tissue structures. The human skull with the installed airway model was scanned eight times using the iCAT CBCT Unit (Imaging Sciences International, Hatfield,

Pennsylvania, USA) utilizing the following scanning protocols each with different resolution and scanning time.

Table 1: the selected scanning settings used in the study.

Scans	Voxel size	Scan time
Scan 1	0.2 mm	14.7 seconds
Scan 2	0.2 mm	26.9 seconds
Scan 3	0.25 mm	14.7 seconds
Scan 4	0.25 mm	26.9 seconds
Scan 5	0.3 mm	4.7 seconds
Scan 6	0.3 mm	8.9 seconds
Scan 7	0.4 mm	4.7 seconds
Scan 8	0.4 mm	8.9 seconds

The scan data were uploaded to Dolphin3D imaging software (version 11.95; Dolphin Imaging & Management Solutions, Chatworth, California, USA). The same software was used then to orient and measure the airway volume, skeletal and dental parameters. 3D images were orientated by adjusting the Frankfort horizontal Plane (FHP) parallel to the floor from the sagittal view and the midsagittal plane perpendicular to the FHP from the frontal view figures 4 - 6.

The same software was used to measure and calculate all the selected airway, skeletal, and dental parameters. The airway volume was measured after tracing the boundaries of the airway model where the software then filled and calculated airway area in cubic millimeter at different segmentation levels (S) from S10 – S80. The minimum segmentation level in this study was set at S10 with increments of S5 until the maximum segmentation level was reached at S80. This process was repeated for all scanning data figures 7 - 10.

The selected skeletal and dental parameters were measured in vertical and sagittal dimensions on the 3D images and sagittal slices of the CBCT images. On the 3D images, a line was drawn from the head of the condyle to the coronoid process representing the anterior posterior measurement

while for the vertical measurement, a line was drawn from the head of condyle to the Gonion point on the right side representing the ramus length figure 11.

On the sagittal slices, maxillary length was drawn as a line from anterior nasal spine to posterior nasal spine representing the anterior posterior measurement while for the vertical measurement, lower anterior facial height (LAFH) was drawn as a line from the anterior nasal spine to the pogonion point figure 12. The dental measurements were performed by measuring the length and width of the maxillary right central incisor (UR1). The length of the UR1 was measured from the middle of the incisal edge to the root apex. The width was measured between the height of contours of the mesial and distal marginal ridges figure 13.

4.1 Statistical methods and reliability test

All selected parameters of airway volume, skeletal, and dental measurements were recorded 8 times for each scanning resolution over 64 days by the primary investigator (WA) and repeated after an interval period of 2 weeks by the same investigator to measure the intra-reliability test. The same measurements were recorded one more time by the main investigator (AG) using the same protocol to measure the inter-reliability test. The measurement errors were assessed by Dahlberg's method (Dahlberg, 1940) and the intraclass correlation coefficient (ICC) was used to assess intra-examiner reliability. The measurements were normally distributed; the mean and standard deviation were calculated and compared using Mann-Whitney test. $P \leq 0.05$ was considered statistically significant.

All statistical calculations were done using the computer programs Microsoft Excel 2010 (Microsoft Corporation, New York, New York, USA) and Statistical Package for the Social Sciences software (version 15; SPSS, Chicago, Illinois, USA).

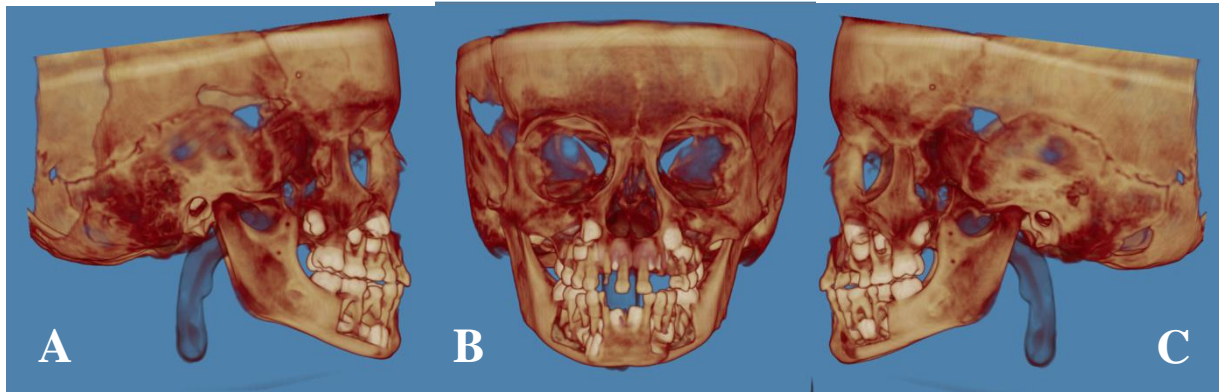


Figure 4 : 3D CBCT skull volume A) right side, B) frontal view, and C) left side.

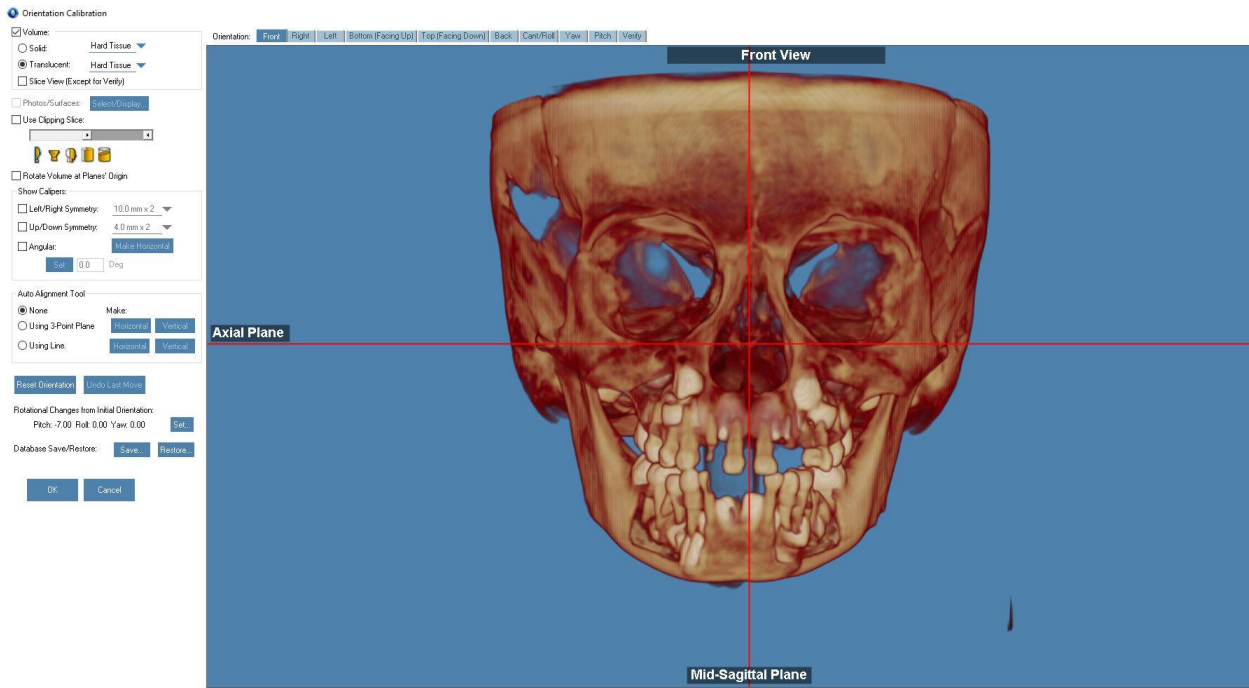


Figure 5: 3D CBCT image orientation: frontal view. The midsagittal plane was adjusted on the skeletal midline of the face.

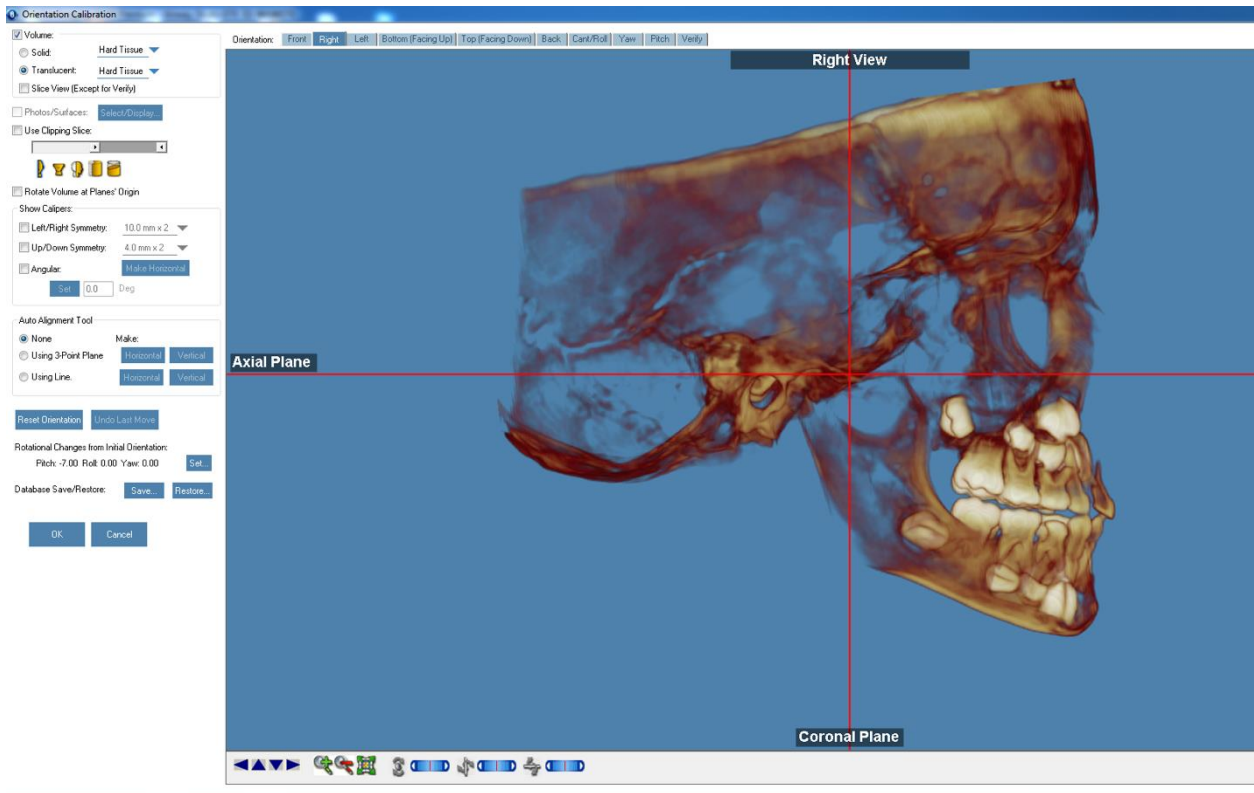


Figure 6: Image orientation: sagittal views, the axial plane was lined up with the Frankfort horizontal plane.

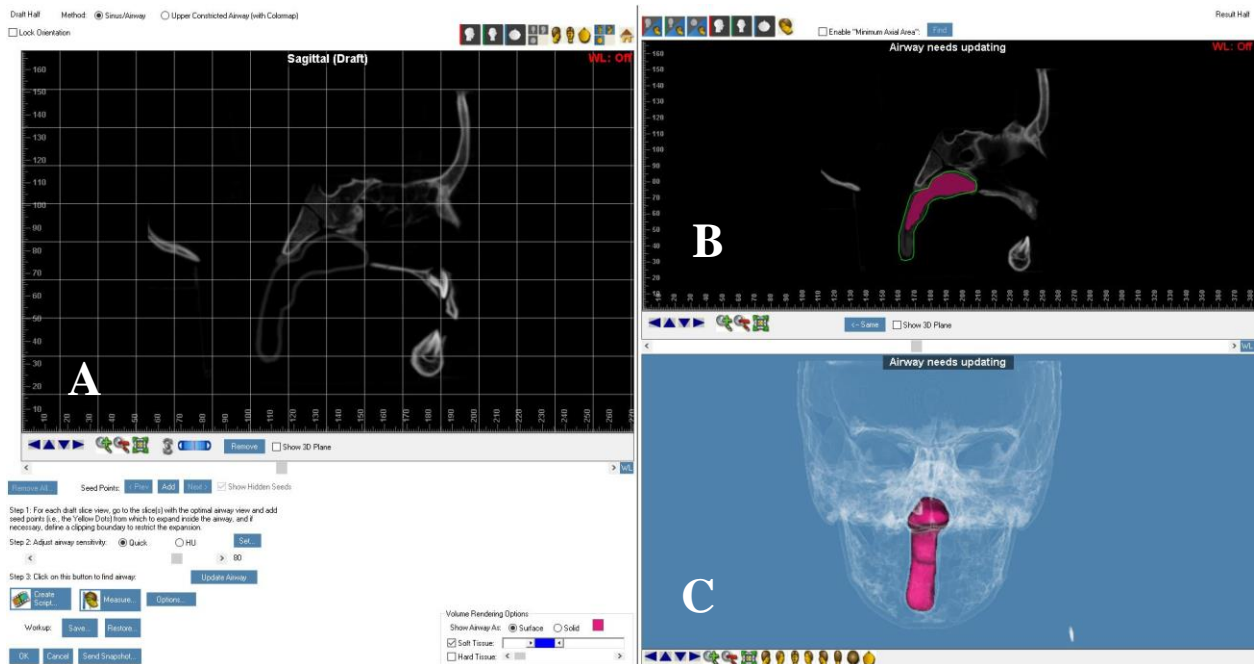


Figure 7: A) sagittal section, (B) sagittal section showing airway surface area, C) 3D view showing airway volume.

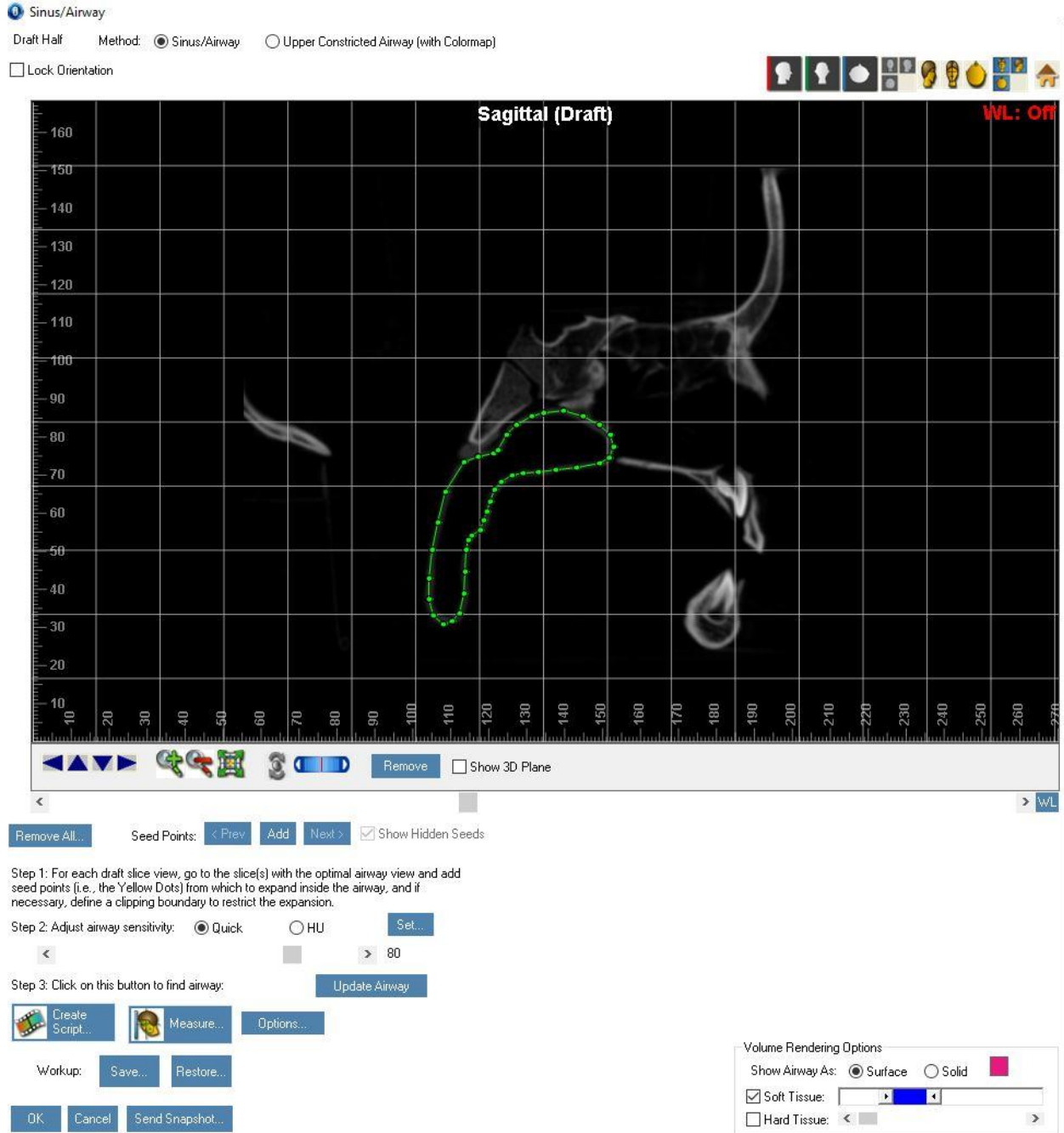


Figure 8: The airway boundaries traced on the midsagittal section.

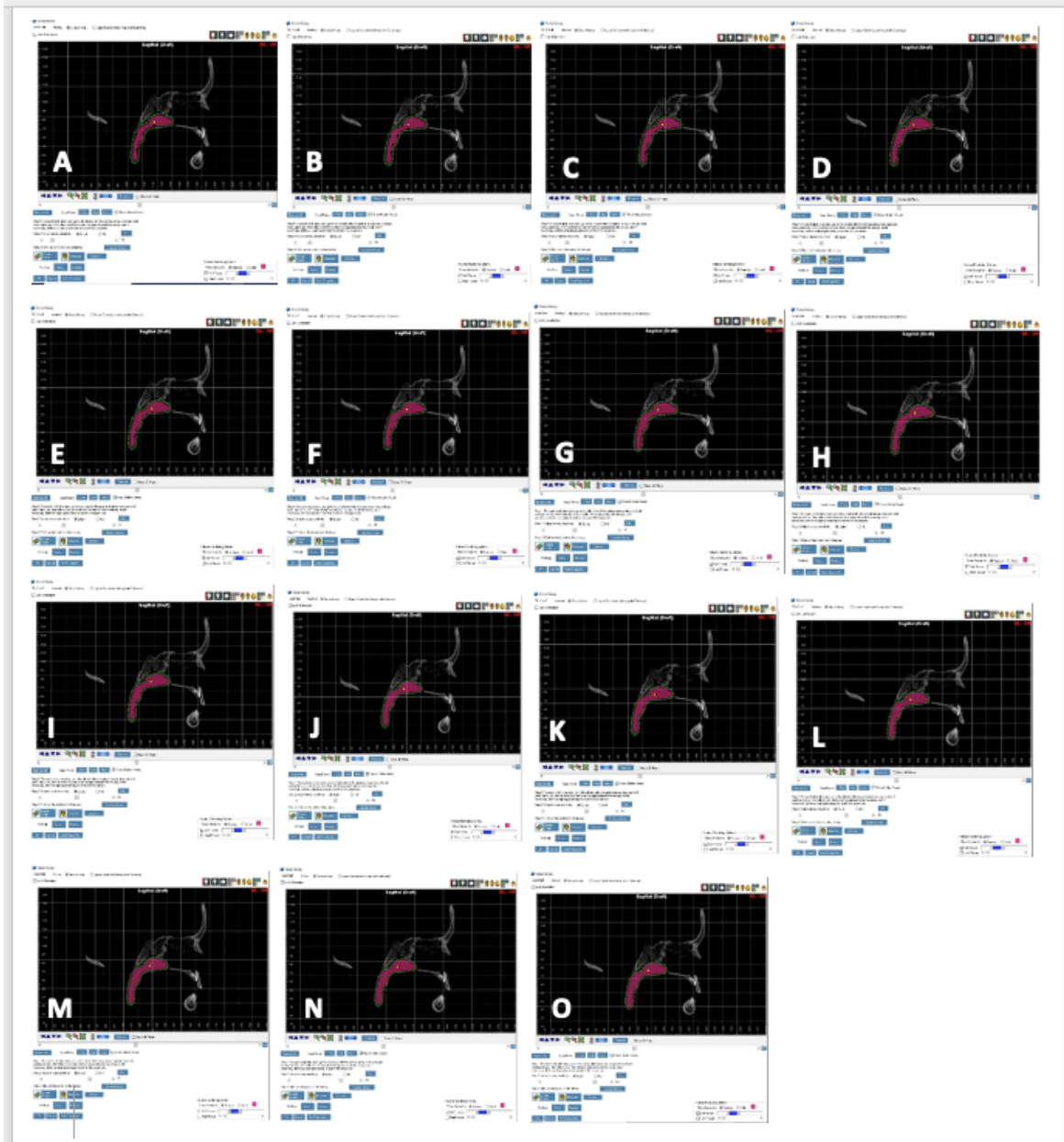


Figure 9 : The Airway was segmented at different levels starting from S10 to S80 with increasing increment of S5 between each level.

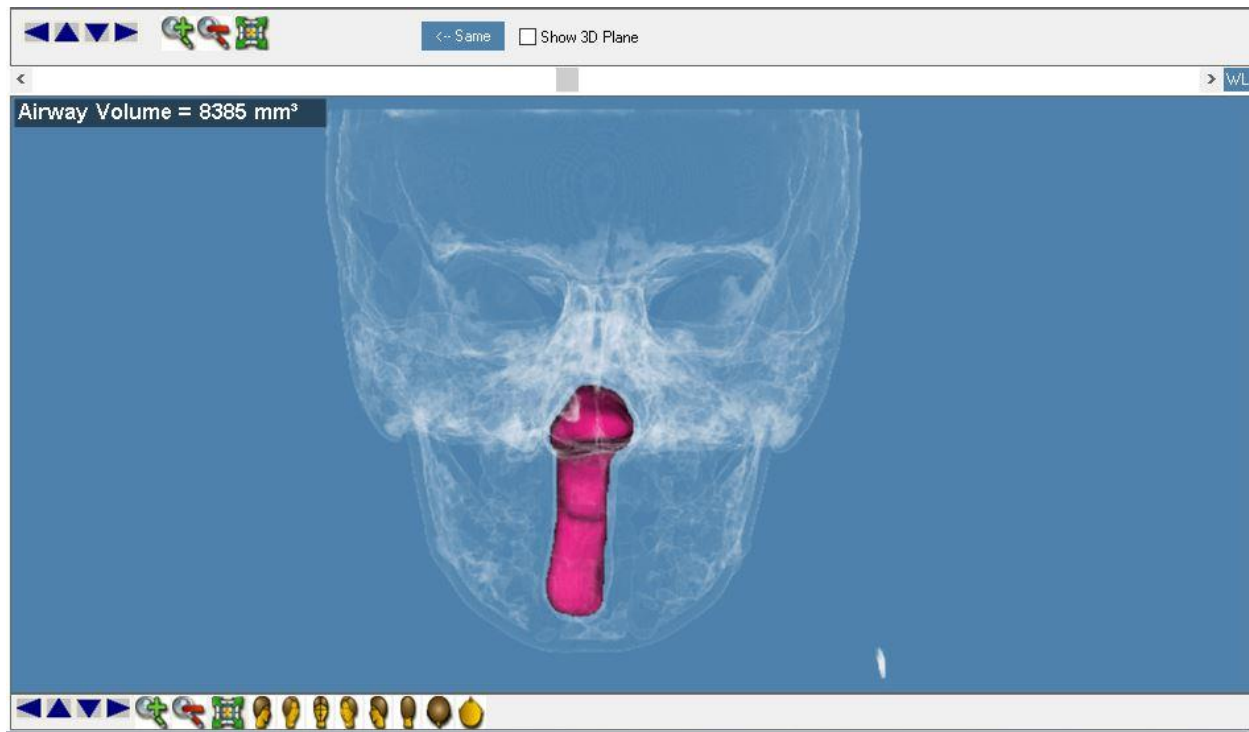


Figure 10: 3D image showing the airway volume.

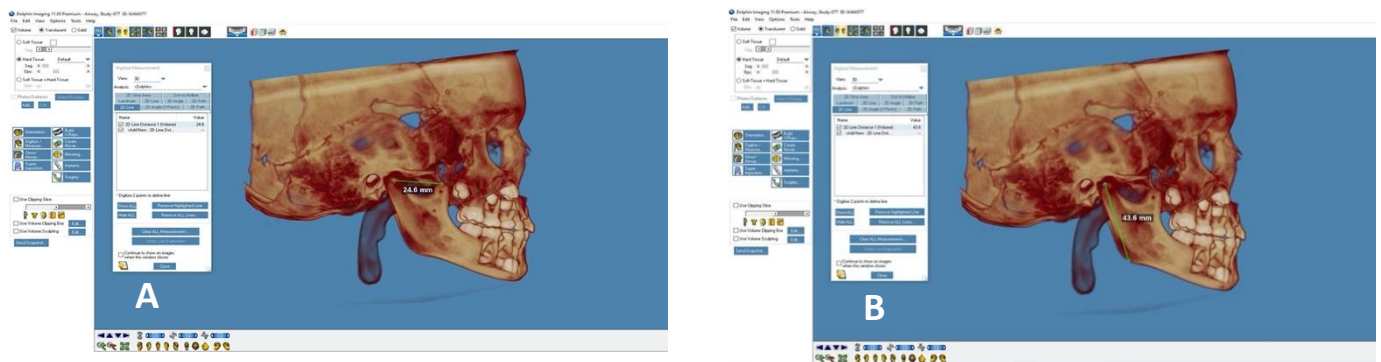


Figure 11 : 3D image showing the A) the distance between the head of condyle to the coronoid process, and (B) the distance between the head of condyle to Gonion point.

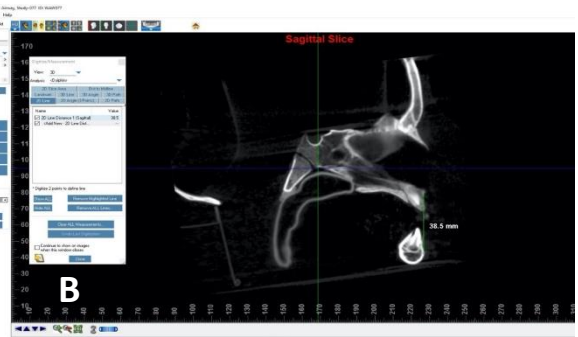


Figure 12: CBCT sagittal section showing the A) maxillary length, and B) the lower anterior facial height.

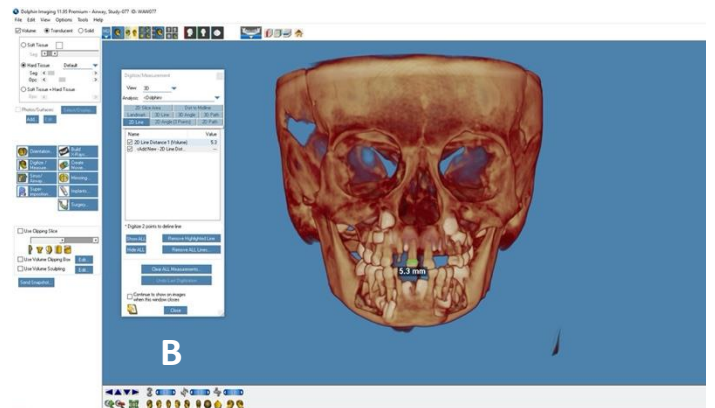


Figure 13: 3D image showing A) the length and B) width of UR1

5. RESULTS

The intra- and inter-examiner reliability tests showed no statistically significant differences between readings and excellent intra-examiner reliability for all measurements (Tables 2).

Comparison of airway volume between 14.7 and 26.9 seconds showed statistically significant differences among the different segmentation levels S10 - S80 at 0.2 and 0.25 voxel sizes, respectively (Table 3).

Comparison of airway volume between 4.7 and 8.9 seconds showed statistically significant differences among the different segmentation levels S10 – S50 at 0.3 voxel size however, there was no statistically significant differences detected at 0.4 voxel size (Table 4).

No statistically significant changes were found in the skeletal and dental parameters between 14.7 and 26.9 seconds at 0.2 voxel size except for the ramus length. However, all skeletal and dental parameters showed significant differences at 0.25 voxel size (Table 5).

No statistically significant changes were found in all skeletal and dental parameters between 4.7 and 8.9 seconds at 0.3 and 0.4 voxel sizes, respectively except for UR1 length and UR1 width were statistically significant different between 4.7 and 8.9 seconds at 0.4 voxel size (Table 6).

Comparison of airway volume between different voxel sizes of 0.2 and 0.25 showed statistically significant differences among the different segmentation levels S10 - S80 at 14.7 and 26.9 seconds, respectively (Table 7).

Comparison of airway volume between different voxel sizes of 0.3 and 0.4 showed statistically significant differences among the different segmentation levels S10 – S50 at 4.7 and 8.9 seconds, respectively. (Table 8).

No statistically significant changes were found in all skeletal and dental parameters between 0.2 and 0.25 voxel sizes at 14.7 and 26.9 seconds except for the ramus length which was statistically significant different between 0.2 and 0.25 voxel sizes at 26.9 seconds (Table 9).

No statistically significant changes were found in all skeletal and dental parameters between 0.3 and 0.4 voxel sizes at 4.7 and 8.9 seconds (Table 10).

By comparing the four different resolutions selected in this study (0.2, 0.25, 0.3, and 0.4 voxel sizes) and eliminating the time, statistically significant differences have been found in the airway volume measurements at all airway segmentation levels except S35, S40, S45, and S50 (Table 11). However, the skeletal and dental parameters did not show any significant differences except for the ramus length (P-value: 0.05).

Table 2: Interrater reliability

	Investigators	N	Mean	Std. Deviation	P-value
A10	AG	64	6483.00	249.140	1.0
	WA	64	6483.00	249.140	
A15	AG	64	6750.13	260.085	1.0
	WA	64	6750.13	260.085	
A20	AG	64	6981.00	265.942	1.0
	WA	64	6981.00	265.942	
A25	AG	64	7170.63	269.072	1.0
	WA	64	7170.63	269.072	
A30	AG	64	7335.00	275.355	1.0
	WA	64	7335.00	275.355	
A35	AG	64	7485.25	286.698	1.0
	WA	64	7485.25	286.698	
A40	AG	64	7635.00	308.218	1.0
	WA	64	7635.00	308.218	
A45	AG	64	7784.25	348.175	1.0
	WA	64	7784.25	348.175	
A50	AG	64	7937.75	400.966	1.0
	WA	64	7937.75	400.966	
A55	AG	56	7976.57	364.263	1.0
	WA	56	7976.57	364.263	
A60	AG	48	7961.00	171.098	1.0
	WA	48	7961.00	171.098	
A65	AG	48	8076.17	150.454	1.0
	WA	48	8076.17	150.454	
A70	AG	48	8192.67	131.211	1.0
	WA	48	8192.67	131.211	
A75	AG	48	8314.00	115.532	1.0
	WA	48	8314.00	115.532	
A80	AG	48	8439.67	101.679	1.0
	WA	48	8439.67	101.679	

Table 3: Comparison of airway volume measurements showing the effect of different scanning time (14.7 and 26.9 seconds) on the same voxel size.

Airway volume at different resolutions and scanning time						
Airway segmentation level	Airway volume at 0.2 Vox size		P Value	Airway volume at 0.25 Vox		P Value
	14.7 sec	26.9 sec		14.7 sec	26.9 sec	
	Mean (SD)	Mean (SD)		Mean (SD)	Mean (SD)	
S10	6567(0)	6715(0)	<0.001*	6578(0)	6772(0)	<0.001*
S15	6801(0)	6973(0)	<0.001*	6821(0)	7036(0)	<0.001*
S20	7016(0)	7193(0)	<0.001*	7042(0)	7242(0)	<0.001*
S25	7204(0)	7365(0)	<0.001*	7233(0)	7411(0)	<0.001*
S30	7372(0)	7497(0)	<0.001*	7392(0)	7552(0)	<0.001*
S35	7507(0)	7609(0)	<0.001*	7531(0)	7665(0)	<0.001*
S40	7628(0)	7709(0)	<0.001*	7649(0)	7770(0)	<0.001*
S45	7727(0)	7808(0)	<0.001*	7747(0)	7867(0)	<0.001*
S50	7818(0)	7905(0)	<0.001*	7836(0)	7966(0)	<0.001*
S55	7909(0)	8003(0)	<0.001*	7923(0)	8068(0)	<0.001*
S60	7999(0)	8102(0)	<0.001*	8015(0)	8015(0)	<0.001*
S65	8097(0)	8200(0)	<0.001*	8015(0)	8269(0)	<0.001*
S70	8199(0)	8299(0)	<0.001*	8206(0)	8370(0)	<0.001*
S75	8299(0)	8404(0)	<0.001*	8315(0)	8477(0)	<0.001*
S80	8431(0)	8513(0)	<0.001*	8433(0)	8585(0)	<0.001*

Significant at $P \leq 0.05$.

Table 4: Comparison of airway volume measurements showing the effect of different scanning time (4.7 and 8.9 seconds) on the same voxel size.

	0.3 Vox		P Value	0.4 Vox		P Value
	4.7 sec	8.9 sec		4.7 sec	8.9 sec	
	Mean (SD)	Mean (SD)		Mean (SD)	Mean (SD)	
S10	6494(0)	6065(0)	<0.001*	6579(-)	6320(250.45)	0.317
S15	6800(0)	6304(0)	<0.001*	6920(-)	6613(296.41)	0.317
S20	7069(0)	6511(0)	<0.001*	7198(-)	6866(320.68)	0.317
S25	7282(0)	6686(0)	<0.001*	7416(-)	7070(334.62)	0.317
S30	7479(0)	6828(0)	<0.001*	7623(-)	7257(354.24)	0.317
S35	7683(0)	6970(0)	<0.001*	7840(-)	7433(394.01)	0.317
S40	7911(0)	7105(0)	<0.001*	8082(-)	7625(442.03)	0.317
S45	8166(0)	7239(0)	<0.001*	8354(-)	7827(510.20)	0.317
S50	8437(0)	7379(0)	<0.001*	8645(-)	8042(583.01)	0.317

Significant at $P \leq 0.05$.

Table 5: Comparison of skeletal and dental measurements showing the effect of different scanning time (14.7 and 26.9 seconds) on the same voxel size.

	0.2 Vox		P Value	0.25 Vox		P Value
	14.7 sec	26.9 sec		14.7 sec	26.9 sec	
	Mean (SD)	Mean (SD)		Mean (SD)	Mean (SD)	
Ramus length	43.68(0.08)	43.80(0.09)	0.013*	43.70(0.11)	43.67(0.04)	<0.001*
Condyle-coronoid distance	24.62(0.04)	24.62(0.07)	0.902	24.58(0.03)	24.60(0.05)	<0.001*
LAFH	38.22(0.04)	38.22(0.07)	0.643	38.16(0.07)	38.25(0.13)	<0.001*
Maxillary length	38.40(0)	38.40(0)	1.000	38.41(0.03)	38.37(0.04)	<0.001*
UL1 width	5.21(0.03)	5.18(0.06)	0.333	5.21(0.03)	5.21(0.03)	<0.001*
UL1 length	14.13(0.07)	14.12(0.07)	0.589	14.12(0.04)	14.15(0.07)	<0.001*

Significant at $P \leq 0.05$.

Table 6: Comparison of skeletal and dental measurements showing the effect of different scanning time (4.7 and 8.9 seconds) on the same voxel size.

	0.3 Vox		P Value	0.4 Vox		P Value
	4.7 sec	8.9 sec		4.7 sec	8.9 sec	
	Mean (SD)	Mean (SD)		Mean (SD)	Mean (SD)	
Ramus length	43.70(0.05)	43.66(0.10)	0.565	43.70	43.70(0)	1.000
Condyle-coronoid distance	24.61(0.03)	24.58(0.03)	0.171	24.60	24.59(0.02)	0.796
LAFH	38.22(0.07)	38.20(0)	0.317	38.20	38.20(0.05)	1.000
Maxillary length	38.40(0)	38.40(0)	1.000	38.40	38.40(0.04)	0.873
UL1 width	5.22(0.04)	5.17(0.04)	0.053	5.30	5.19(0.02)	0.005*
UL1 length	14.11(0.03)	14.15(0.07)	0.239	14.20	14.10(0.02)	0.008*

Significant at $P \leq 0.05$.

Table 7: The effect of different voxel sizes (0.2 vox and 0.25 vox) on the airway volume measurements using the same scanning time.

	14.7 sec		P Value	26.9 sec		P Value
	0.2 Vox	0.25 Vox		0.2 Vox	0.25 Vox	
	Mean (SD)	Mean (SD)		Mean (SD)	Mean (SD)	
S10	6567(0)	6578(0)	<0.001*	6715(0)	6772(0)	<0.001*
S15	6801(0)	6821(0)	<0.001*	6973(0)	7036(0)	<0.001*
S20	7016(0)	7042(0)	<0.001*	7193(0)	7242(0)	<0.001*
S25	7204(0)	7233(0)	<0.001*	7365(0)	7411(0)	<0.001*
S30	7372(0)	7392(0)	<0.001*	7497(0)	7552(0)	<0.001*
S35	7507(0)	7531(0)	<0.001*	7609(0)	7665(0)	<0.001*
S40	7628(0)	7649(0)	<0.001*	7709(0)	7770(0)	<0.001*
S45	7727(0)	7747(0)	<0.001*	7808(0)	7867(0)	<0.001*
S50	7818(0)	7836(0)	<0.001*	7905(0)	7966(0)	<0.001*
S55	7909(0)	7923(0)	<0.001*	8003(0)	8068(0)	<0.001*
S60	7999(0)	8015(0)	<0.001*	8102(0)	8166(0)	<0.001*
S65	8097(0)	8107(0)	<0.001*	8200(0)	8269(0)	<0.001*
S70	8199(0)	8206(0)	<0.001*	8299(0)	8370(0)	<0.001*
S75	8310(0)	8315(0)	<0.001*	8404(0)	8477(0)	<0.001*
S80	8431(0)	8433(0)	<0.001*	8513(0)	8585(0)	<0.001*

Significant at $P \leq 0.05$.

Table 8: The effect of different voxel sizes (0.3 vox and 0.4 vox) on the airway volume measurements using the same scanning time.

	4.7 sec		P Value	8.9 sec		P Value
	0.3 Vox	0.4 Vox		0.3 Vox	0.4 Vox	
	Mean (SD)	Mean (SD)		Mean (SD)	Mean (SD)	
S10	6494(0)	6579(0)	<0.001*	6065(0)	6094(0)	<0.001*
S15	6800(0)	6920(0)	<0.001*	6304(0)	6346(0)	<0.001*
S20	7069(0)	7198(0)	<0.001*	6511(0)	6577(0)	<0.001*
S25	7282(0)	7416(0)	<0.001*	6686(0)	6768(0)	<0.001*
S30	7479(0)	7623(0)	<0.001*	6828(0)	6937(0)	<0.001*
S35	7683(0)	7840(0)	<0.001*	6970(0)	7077(0)	<0.001*
S40	7911(0)	8082(0)	<0.001*	7105(0)	7226(0)	<0.001*
S45	8166(0)	8354(0)	<0.001*	7239(0)	7366(0)	<0.001*
S50	8437(0)	8645(0)	<0.001*	7379(0)	7516(0)	<0.001*

Significant at $P \leq 0.05$.

Table 9: Comparison of Skeletal measurements for the time 14.7 sec and 26.9 sec between two different resolutions (0.2vox and 0.25 vox)

	14.7 sec		P Value	26.9 sec		P Value
	0.2 Vox	0.25 Vox		0.2 Vox	0.25Vox	
	Mean (SD)	Mean (SD)		Mean (SD)	Mean (SD)	
Ramus length	43.68(0.08)	43.70(0.11)	0.904	43.80(0.1)	43.67(0.04)	0.003*
Condyle-coronoid distance	24.62(0.04)	24.58(0.03)	0.090	24.62(0.07)	24.60(0.05)	0.393
LAFH	38.22(0.04)	38.16(0.07)	0.053	38.22(0.07)	38.25(0.13)	0.890
Maxillary length	38.40(0)	38.41(0.03)	0.721	38.40(0)	38.40(0.04)	0.143
UL1 width	5.21(0.03)	5.21(0.03)	1.000	5.18(0.06)	5.21(0.03)	0.333
UL1 length	14.13(0.07)	14.12(0.04)	0.890	14.12(0.07)	14.15(0.07)	0.333

Significant at $P \leq 0.05$.

Table 10: Comparison of Skeletal measurements for the time 4.7 sec & 8.9 sec between two different resolution (0.3vox & 0.4 vox)

	4.7 sec		P Value	8.9 sec		P Value
	0.3 Vox	0.4 Vox		0.3 Vox	0.4 Vox	
	Mean (SD)	Mean (SD)		Mean (SD)	Mean (SD)	
Ramus length	43.70(0.05)	43.70(0)	1.000	43.66(0.10)	43.70(0)	0.537
Condyle-coronoid distance	24.61(0.03)	24.60(0)	0.317	24.58(0.035)	24.58(0.03)	1.000
LAFH	38.22(0.07)	38.18(0.03)	0.171	38.20(0)	38.22(0.07)	0.317
Maxillary length	38.40(0)	38.40(0)	1.000	38.40(0)	38.40(0.44)	0.537
UL1 width	5.22(0.04)	5.20(0.05)	0.332	5.17(0.04)	5.20(0)	0.143
UL1 length	14.11(0.03)	14.11(0.03)	1.000	14.11(0.07)	14.13(0.06)	0.239

Significant at $P \leq 0.05$.

Table11: Comparison of airway volume measurements between different resolution regardless the time

	0.2 Vox	0.25 Vox	0.3 Vox	0.4 Vox	P-value
	Mean (SD)	Mean (SD)	Mean (SD)	Mean (SD)	
S10	6641.00(76.42)	6675.00(100.18)	6279.50(221.53)	6336.50(250.45)	<0.001*
S15	6887.00(88.82)	6928.50(111.02)	6552.(256.13)	6633.00(296.41)	<0.001*
S20	7104.50(91.40)	7142(103.28)	6790(288.15)	6887.50(320.68)	<0.001*
S25	7284.50(83.14)	7322(91.91)	6984(307.77)	7092.00(334.62)	<0.001*
S30	7434.50(64.55)	7472(82.62)	7153.50(336.17)	7280(354.24)	<0.001*
S35	7558(52.67)	7598(69.19)	7326.50(368.19)	7458(394.01)	0.392
S40	7668.50(41.82)	7709.50(62.48)	7508(416.21)	7654 (442.03)	0.392
S45	7767.50(41.82)	7807(61.96)	7702.50(478.70)	7860(510.20)	0.392
S50	7861.50(44.92)	7901(67.13)	7908(546.34)	8080(583.01)	0.392
S55	7956(48.54)	7995.50(74.87)	8134(632.07)	7665(0)	0.008*
S60	8050(53.18)	8090.50(77.97)	7672(0)	7812(0)	<0.001*
S65	8148.50(53.18)	8188(83.65)	7817(0)	7967(0)	<0.001*
S70	8249(51.64)	8288(84.68)	7963(0)	8119(0)	<0.001*
S75	8357(48.54)	8396(83.65)	8110(0)	8268(0)	<0.001*
S80	8472(42.34)	8509(78.49)	8256(0)	8420(0)	<0.001*

Significant at $P \leq 0.05$.

Table12: Comparison of Skeletal measurements between different resolution regardless the time

	0.2 Vox	0.25 Vox	0.3 Vox	0.4 Vox	P-value
	Mean (SD)	Mean (SD)	Mean (SD)	Mean (SD)	
Ramus length	43.74(0.10)	43.68(0.08)	43.68(0.08)	43.70(0)	0.05*
Condyle-coronoid distance	24.62(0.05)	24.59(0.04)	24.60(0.03)	24.59(0.02)	0.125
LAFH	38.22(0.05)	38.20(0.11)	38.21(0.05)	38.20(0.05)	0.441
Maxillary length	38.40(0)	38.39(0.04)	38.40(0)	38.40(0.04)	0.726
UL1 width	5.20(0.05)	5.21(0.03)	5.20(0.05)	5.20(0.03)	0.810
UL1 length	14.13(0.07)	14.138(0.06)	14.131(0.06)	14.11(0.05)	0.628

Significant at $P \leq 0.05$.

6. DISCUSSION

Cone-beam computed tomography (CBCT) has been widely used in orthodontics since its introduction in dentistry in 1998. Applications of CBCT images in orthodontics include dental measurements, evaluation of root resorption, diagnoses of the temporomandibular joint, airway assessment, 3D cephalometry, and evaluation of orthognathic surgery (Abdelkarim, 2019). The image quality of CBCT scan might be influenced by a number of variables, such as the scanning unit, scanning time, and scanning resolution defined by the voxel size (Lohrabian et al., 2019). CBCT volumetric data set is composed of volume elements called voxels and the dimension of each voxel determines spatial resolution of the image. Images acquired in smaller voxel sizes have better spatial resolution (Yılmaz et al., 2017).

CBCT shows great promise of becoming a useful tool for both patient management and research. However, if it is to be relied on, the accuracy of the three-dimensional (3D) reconstructions coming from 3D images needs to be clearly established. Accuracy has already been assessed by comparing reconstructions using CBCT with those provided by the standard in 3D dental research, micro-CT (Rasteau et al., 2020). Similar volumetric measurements were obtained using CBCT with anisotropic voxel size of 76 mm and the reference method, micro-CT, with an isotropic voxel size of 41 mm (Whittier et al., 2020). The important influence of voxel size on the quality of CBCT images and on scanning and reconstruction times is already acknowledged. However, data are still lacking on the effects of voxel size on the metric accuracy of reconstructions (Tayman et al., 2019).

The use of an airway model for evaluating accuracy and reliability of volumetric measurements in the present study eliminated the great variability that may occur when using CBCTs of a real human airway. The variability results from changes in the airway position, morphology, and dimension due to the effects of either the patient's respiration or swallowing actions during the

scanning procedure (Sin et al., 2021). Landmark-based analysis of maxillofacial structure with linear and angular measurements is the most common method of cephalometric analysis in orthodontics since Broadbent introduced cephalometric radiography. However, in the literature, few studies so far have assessed the effect of voxel size on the accuracy of landmark identification in the CBCT images (Lee et al., 2019).

Evaluation of the airway is useful in some orthodontic patients especially those with breathing disorders. The CBCT has been recently established as an orthodontic diagnostic modality. It has the advantage of high quality images and superior anatomic presentation with less radiation doses than the conventional CTs (Behrents et al., 2019). The purpose of this study was to evaluate the accuracy and reliability of the airway volume, dental, and skeletal parameters measured digitally on cone beam computed tomography scans (CBCTs) using airway model scanned with different resolutions and timings.

While many previous studies investigated the reliability of CBCT measurements of craniofacial and dental parameters, the literature is deficient in evaluating the reliability of airway measurements. Lagravère et al., (2008) and Baumgaertel et al., (2009) compared dental measurements generated on CBCT scans to the measurements made on a co-ordinate measuring machine using a synthetic mandible and to the measurements made directly on the dentitions of human dry skulls, respectively. Their results indicated that the CBCT measurements were reliable and accurate and supported the use of CBCT technology to analyze the dentition. Studies concerning the reliability of the airway measurements on CBCTs compared them with data obtained from two-dimensional cephalograms. Aboudara et al., (2003) compared airway information from 11 normal adolescent children between lateral cephalometric headfilms and three-dimensional CBCTs. They concluded that intra subject proportion of airway volume to area shows

moderate variability and that CT airway volume shows more variability than corresponding headfilm airway area. They also indicated that there may be airway information that is not accurately depicted on the lateral headfilm. In their later study, Aboudara et al. (2009) compared imaging information about airway size between lateral cephalometric head films and three-dimensional CBCTs from 35 adolescent subjects.

In agreement with the current study, Ghoneima and Kula (2013) reported that no significant statistical difference was found between the airway volumes. In our study, no significant differences were also found in airway volume using the same resolution and same scanning time. However, significant differences were found when compared the airway volume at different resolution and scanning time indicating a great variability between the different voxel sizes selected in this study (0.2, 0.25, 0.3, and 0.4) as well as the scanning time (4.7, 8.9, 14.7, and 26.9).

In contrast to our results, Alves Jr et al. (2012) reported that the volumes measured with the threshold values of the 25 and 50 filters had statistically significant differences from the gold standard. However, volumes measured with the threshold values of the 70, 71, 72, 73, 74, and 75 showed no statistically significant differences from the gold standard and among them. The gold standard method used to obtain the actual volume of the airway prototype was the volume of water necessary to fill the empty space of the prototype measured by high-precision micropipette of 2 to 20 mL. In our study we found that by using Mann-Whitney test in Airway volume measurements, high significant differences were shown between the scanning time of 14.7 sec, 26.9 sec and two different resolutions of 0.2 and 0.25 voxel sizes. This test was high significant on total and per each resolution, high significant differences were shown between the time 4.7 sec, 8.9 sec and two different resolutions of 0.3 and 0.4 voxel size.

While Maret et al. (2012) showed that the reconstructions from volumetric measurements at 200 mm and 300 mm were compared with those obtained with CBCT, using a voxel size of 76 mm, and micro-CT, voxel size of 41 mm, considered as references. We showed in an earlier study that the volumes obtained with CBCT 76 mm were similar to those from micro-CT 41 mm. Segmentation requires thorough knowledge of the images to be analysed and of the information to be extracted subsequently. Maret et al. (2012) assessed the effect of voxel size on the accuracy of 3D reconstruction of CBCT data. They found that volumetric measurements at voxel size of 200 μm and 300 μm were underestimated by comparing with those obtained with voxel size of 76 μm and 41 μm , Damstra et al., (2010) suggested that there was no statistically significant difference of the linear measurement accuracy between 0.40 mm and 0.25 mm voxel size group.

Ashmawy et al. (2017) showed that the difference between the actual physical measurements obtained by the digital caliber and CBCT measurements was considered as the measurement error and by comparing this error between the CBCT scans (0.2 mm, 0.3 mm, and 0.4 mm voxel size), there was no statistically significant difference between these CBCT scans regarding all measurements except one measurement at the 0.4 mm voxel size CBCT scan showed a statistically significant high mean error; while all other measurements showed no statistically significant difference between the CBCT measurements and actual physical measurements.

In the present study, Using Mann-Whitney test in skeletal measurements, significant differences were shown between the time 26.9 sec and two different resolutions of 0.2 and 0.25 voxel sizes as regard to the ramus length measured on the 3D volume. Although ramus length was significant at 26.9 second, no significant differences were shown between the time 4.7 sec, 8.9 sec and two different resolutions of 0.3 and 0.4 voxel sizes. This test was significant in all skeletal and dental parameters the two different scanning time of 14.7 and 26.9 second at 0.25 voxel size.

In the present study according to comparison of airway volume measurements between different resolutions after eliminating the time as a factor, we found that high significant differences were shown between airway volume measurements among the different segmentation levels except from A30 to A50. Likewise, skeletal parameters did not show statistical significant differences among the different resolutions after eliminating the time as a factor except for the ramus height.

7. CONCLUSIONS

This study confirms that reliability of the CBCT measurements in airway volume, skeletal and dental parameters. Airway volume measurements vary based on the voxel size, scanning time and segmentation level of CBCT scans. Clinicians and researchers should be aware of the effect of the scanning resolution, scanning time, and segmentation level on the airway measurements since this could affect the clinical judgement. This study recommends the clinicians to use the same scanning settings before and after treatment while performing radiographic examinations for critical cases.

8. REFERENCES

- Abdelkarim, A. (2019). Cone-beam computed tomography in orthodontics. *Dentistry journal*, 7(3), 89.
- Aboudara, C., Hatcher, D., Nielsen, I., & Miller, A. (2003). A three-dimensional evaluation of the upper airway in adolescents. *Orthodontics Craniofacial Research*, 6, 173-175.
- Aboudara, C., Nielsen, I., Huang, J. C., Maki, K., Miller, A. J., & Hatcher, D. (2009). Comparison of airway space with conventional lateral headfilms and 3-dimensional reconstruction from cone-beam computed tomography. *American Journal of Orthodontics Dentofacial Orthopedics*, 135(4), 468-479.
- Adarsh, K., Sharma, P., & Juneja, A. (2018). Accuracy and reliability of tooth length measurements on conventional and CBCT images: An in vitro comparative study. *Journal of Orthodontic Science*, 7.
- Aksoy, C., Elsürer, Ç., Artaç, H., & Bozkurt, M. K. (2018). Evaluation of olfactory function in children with seasonal allergic rhinitis and its correlation with acoustic rhinometry. *International Journal of Pediatric Otorhinolaryngology*, 113, 188-191.
- Al-Qawasmi, R., Swiderski, B., & Kaczynski, R. (2020). Evaluating interactions of airway changes during growth with orthodontic treatment. *Int Orthod*, 18(3), 461-467. doi:10.1016/j.ortho.2020.06.005
- AlKawari, H. M., AlBalbeesi, H. O., Alhendi, A. A., Alhuwaish, H. A., Al Jobair, A., & Baidas, L. (2018). Pharyngeal airway dimensional changes after premolar extraction in skeletal class II and class III orthodontic patients. *Journal of Orthodontic Science*, 7.

- Alsufyani, N. A., Noga, M. L., Witmans, M., & Major, P. W. (2017). Upper airway imaging in sleep-disordered breathing: role of cone-beam computed tomography. *Oral Radiology*, 33(3), 161-169.
- Alves Jr, M., Baratieri, C., Mattos, C. T., Brunetto, D., da Cunha Fontes, R., Santos, J. R. L., & de Oliveira Ruellas, A. C. (2012). Is the airway volume being correctly analyzed? *American Journal of Orthodontics Dentofacial Orthopedics*, 141(5), 657-661.
- Amaral, J. L., Lopes, A. J., Veiga, J., Faria, A. C., & Melo, P. L. (2017). High-accuracy detection of airway obstruction in asthma using machine learning algorithms and forced oscillation measurements. *Computer Methods Programs in Biomedicine*, 144, 113-125.
- Ashmawy, M. S., Abou-Khalaf, A. A., & Mostafa, R. A. (2017). Effect of Voxel Size On The Accuracy of Nerve Tracing Module of Cone Beam Computed Tomography Images. *Egyptian Dental Journal*, 63(3-July), 2403-2412.
- Aurand, A. M., Dufour, J. S., & Marras, W. S. (2017). Accuracy map of an optical motion capture system with 42 or 21 cameras in a large measurement volume. *Journal of Biomechanics*, 58, 237-240.
- Balamurugan, S. (2019). *Electrophysiological Profile of Myocardium in Obstructive Sleep Apnea*. Kilpauk Medical College, Chennai,
- Ballikaya, E., Dogan, B. G., Onay, O., & Tekcicek, M. U. (2018). Oral health status of children with mouth breathing due to adenotonsillar hypertrophy. *International Journal of Pediatric Otorhinolaryngology*, 113, 11-15.
- Banerjee, D., Shrivastav, D., Kamble, D., Dhannawat, D., & Purva, V. (2020). Lateral Cephalogram and CBCT as a diagnostic aid for analysis of airway-Review Article. *European Journal of Molecular Clinical Medicine*, 7(7), 1802-1808.

- Banko, B., Djukic, V., Milovanovic, J., Kovac, J., Novakovic, Z., & Maksimovic, R. (2014). MRI in evaluation of neoplastic invasion into preepiglottic and paraglottic space. *Auris Nasus Larynx*, 41(5), 471-474.
- Barbic, D., Chenkin, J., Cho, D. D., Jelic, T., & Scheuermeyer, F. X. (2017). In patients presenting to the emergency department with skin and soft tissue infections what is the diagnostic accuracy of point-of-care ultrasonography for the diagnosis of abscess compared to the current standard of care? A systematic review and meta-analysis. *BMJ open*, 7(1).
- Bates, A. J., Higano, N. S., Hysinger, E. B., Fleck, R. J., Hahn, A. D., Fain, S. B., Woods, J. C. (2019). Quantitative assessment of regional dynamic airway collapse in neonates via retrospectively respiratory-gated 1H ultrashort echo time MRI. *Journal of Magnetic Resonance Imaging*, 49(3), 659-667.
- Baumgaertel, S., Palomo, J. M., Palomo, L., & Hans, M. G. (2009). Reliability and accuracy of cone-beam computed tomography dental measurements. *American Journal of Orthodontics Dentofacial Orthopedics*, 136(1), 19-25.
- Behrents, R. G., Shelgikar, A. V., Conley, R. S., Flores-Mir, C., Hans, M., Levine, M., Stockstill, J. W. (2019). Obstructive sleep apnea and orthodontics: an American Association of Orthodontists white paper. *American Journal of Orthodontics Dentofacial Orthopedics*, 156(1), 13-28. e11.
- Belgin, C. A., Colak, M., Adiguzel, O., Akkus, Z., & Orhan, K. (2019). Three-dimensional evaluation of maxillary sinus volume in different age and sex groups using CBCT. *European Archives of Oto-Rhino-Laryngology*, 276(5), 1493-1499.

- Breyer, T., Echternach, M., Arndt, S., Richter, B., Speck, O., Schumacher, M., & Markl, M. (2009). Dynamic magnetic resonance imaging of swallowing and laryngeal motion using parallel imaging at 3 T. *Magnetic Resonance Imaging*, 27(1), 48-54.
- Cao, M. T., Sternbach, J. M., & Guilleminault, C. (2017). Continuous positive airway pressure therapy in obstructive sleep apnea: benefits and alternatives. *Expert Review of Respiratory Medicine*, 11(4), 259-272.
- Cappellette Jr, M., Nagai, L. H. Y., Gonçalves, R. M., Yuki, A. K., Pignatari, S. S. N., & Fujita, R. R. (2017). Skeletal effects of RME in the transverse and vertical dimensions of the nasal cavity in mouth-breathing growing children. *Dental press journal of orthodontics*, 22(4), 61-69.
- Chan, H.-F., Weatherley, N. D., Johns, C. S., Stewart, N. J., Collier, G. J., Bianchi, S. M., & Wild, J. M. (2019). Airway microstructure in idiopathic pulmonary fibrosis: assessment at hyperpolarized ³He diffusion-weighted MRI. *Radiology*, 291(1), 223-229.
- Chan, H.-L., Yuen, H.-M., Au, C.-T., Chan, K. C.-C., Li, A. M., & Lui, L.-M. (2020). Quasi-conformal Geometry based Local Deformation Analysis of Lateral Cephalogram for Childhood OSA Classification. *arXiv e-prints*.
- Chan, L., Kaczynski, R., & Kang, H.-K. (2020). A cross-sectional retrospective study of normal changes in the pharyngeal airway volume in white children with 3 different skeletal patterns from age 9 to 15 years: Part 1. *American Journal of Orthodontics Dentofacial Orthopedics*, 158(5), 710-721.
- Chen, H., Van Eijnatten, M., Aarab, G., Forouzanfar, T., De Lange, J., Van Der Stelt, P., Wolff, J. (2018). Accuracy of MDCT and CBCT in three-dimensional evaluation of the oropharynx morphology. *European Journal of Orthodontics*, 40(1), 58-64.

- Chen, H., Van Eijnatten, M., Wolff, J., De Lange, J., Van Der Stelt, P. F., Lobbezoo, F., & Aarab, G. (2017). Reliability and accuracy of three imaging software packages used for 3D analysis of the upper airway on cone beam computed tomography images. *Dentomaxillofacial Radiology*, 46(6), 20170043.
- Cilluffo, G., Zicari, A. M., Ferrante, G., Malizia, V., Fasola, S., Duse, M., Brindisi, G. (2020). Assessing repeatability and reproducibility of Anterior Active Rhinomanometry (AAR) in children. *BMC medical research methodology*, 20, 1-11.
- da Costa, E. D., Roque-Torres, G. D., Brasil, D. M., Bóscolo, F. N., de Almeida, S. M., & Ambrosano, G. M. B. (2017). Correlation between the position of hyoid bone and subregions of the pharyngeal airway space in lateral cephalometry and cone beam computed tomography. *The Angle Orthodontist*, 87(5), 688-695.
- Damstra, J., Fourie, Z., Slater, J. J. H., & Ren, Y. (2010). Accuracy of linear measurements from cone-beam computed tomography-derived surface models of different voxel sizes. *American Journal of Orthodontics Dentofacial Orthopedics*, 137(1), 16. e11-16. e16.
- David, O.-T., Tuce, R.-A., Munteanu, O., Neagu, A., & Panainte, I. (2017). Evaluation of the influence of patient positioning on the reliability of lateral cephalometry. *La radiologia medica*, 122(7), 520-529.
- Davis, T. A. (2020). Quantitative Performance Characterization of Radiation Dose for a CS9600 Dental Cone Beam Computed Tomography. (Doctoral), Saint Louis University,
- De Felice, F., Di Carlo, G., Saccucci, M., Tombolini, V., & Polimeni, A. (2019). Dental cone beam computed tomography in children: clinical effectiveness and cancer risk due to radiation exposure. *Oncology*, 96(4), 173-178.

- Di Carlo, G., Saccucci, M., Ierardo, G., Luzzi, V., Occasi, F., Zicari, A. M., Polimeni, A. (2017). Rapid maxillary expansion and upper airway morphology: a systematic review on the role of cone beam computed tomography. *BioMed research international*, 2017.
- Downard, M. G., Lee, A. J., Heald, C. J., Anthony, E. Y., Singh, J., & Templeton, T. W. (2021). A Retrospective Evaluation of Airway Anatomy in Young Children and Implications for One-Lung Ventilation. *J Cardiothorac Vasc Anesth*, 35(5), 1381-1387. doi:10.1053/j.jvca.2020.08.015
- Dublin, L. P., McGuigan, M., & Place, L. (2017). An analysis of effective dose optimization and its impact on image quality and diagnostic efficacy relating to dental cone beam computed tomography (CBCT).
- Elders, B., Ciet, P., Tiddens, H., van den Bosch, W., Wielopolski, P., & Pullens, B. (2021). MRI of the upper airways in children and young adults: the MUSIC study. *Thorax*, 76(1), 44-52.
- Eliliwi, M., Bazina, M., & Palomo, J. M. (2020). kVp, mA, and voxel size effect on 3D voxel-based superimposition. *The Angle Orthodontist*, 90(2), 269-277.
- Fokas, G., Vaughn, V. M., Scarfe, W. C., & Bornstein, M. M. (2018). Accuracy of linear measurements on CBCT images related to presurgical implant treatment planning: A systematic review. *Clin Oral Implants Res*, 29, 393-415.
- Friedrich, R. E., Lehmann, J.-M., Rother, J., Christ, G., Zu Eulenburg, C., Scheuer, H. T., & Scheuer, H. A. (2017). A lateral cephalometry study of patients with neurofibromatosis type 1. *Journal of Cranio-Maxillofacial Surgery*, 45(6), 809-820.
- García-Sanz, V., Bellot-Arcís, C., Hernández, V., Serrano-Sánchez, P., Guarinos, J., & Paredes-Gallardo, V. (2017). Accuracy and reliability of Cone-Beam Computed

Tomography for linear and volumetric mandibular condyle measurements. A human cadaver study. *Scientific Reports*, 7(1), 1-8.

- Ghoneima, A., & Kula, K. (2013). Accuracy and reliability of cone-beam computed tomography for airway volume analysis. *The European Journal of Orthodontics*, 35(2), 256-261.
- Grondin, F., Hall, T., von Piekartz, H., & Practice. (2017). Does altered mandibular position and dental occlusion influence upper cervical movement: A cross-sectional study in asymptomatic people. *Musculoskeletal Science*, 27, 85-90.
- Gupta, R., Kaur, S., Mahajan, N., Kotwal, B., Kharyal, S., & Gupta, N. (2017). Prevalence of Subtypes of Long Face Pattern in Jammu Population. *International Journal Of Preventive Public Health Sciences*, 3(2), 22-24.
- Gutiérrez, D. A. R., Garzón, J. S., Franco, J. Q., & Botero-Mariaca, P. (2021). Anterior open bite and its relationship with dental arch dimensions and tongue position during swallowing and phonation in individuals aged 8–16 years: A retrospective case-control study. *International Orthodontics*, 19(1), 107-116.
- Han, B., Liu, Y., Zhang, X., & Wang, J. (2015). Three-dimensional printing as an aid to airway evaluation after tracheotomy in a patient with laryngeal carcinoma. *BMC Anesthesiology*, 16(1), 1-4.
- Han, Y., Tian, Y., Zhang, H., Zhao, Y., Xu, M., & Guo, X. (2018). Radiologic indicators for prediction of difficult laryngoscopy in patients with cervical spondylosis. *Acta Anaesthesiologica Scandinavica*, 62(4), 474-482.

- Hayashi, T., Arai, Y., Chikui, T., Hayashi-Sakai, S., Honda, K., Indo, H., Nagasawa, M. (2018). Clinical guidelines for dental cone-beam computed tomography. *Oral Radiology*, 34(2), 89-104.
- Hekmatian, E., Jafari-Pozve, N., & Khorrami, L. (2014). The effect of voxel size on the measurement of mandibular thickness in cone-beam computed tomography. *Dental research journal*, 11(5), 544.
- Hernández, C. P., & Clari, V. R. (2019). Multidisciplinary approach in a case of hemifacial microsomia: Speech and language pathologist contributions. *Revista de Investigación en Logopedia*, 9(1), 17-27.
- Isidor, S., Di Carlo, G., Cornelis, M. A., Isidor, F., & Cattaneo, P. M. (2018). Three-dimensional evaluation of changes in upper airway volume in growing skeletal Class II patients following mandibular advancement treatment with functional orthopedic appliances. *The Angle Orthodontist*, 88(5), 552-559.
- Jain, K., Gupta, N., Yadav, M., Thulkar, S., & Bhatnagar, S. (2019). Radiological evaluation of airway—What an anaesthesiologist needs to know! *Indian Journal of Anaesthesia*, 63(4), 257.
- Jayashree, G. (2020). Pharyngeal Airway Analysis in relation to Position of Hyoid Bone Using Lateral Cephalometrics. (Masters), Ragas Dental College and Hospital, Chennai. Retrieved from <http://repository-tnmgrmu.ac.in/id/eprint/14515>
- Jullabussapa, N., Khwanngern, K., Pateekhum, C., Angkurawaranon, C., & Angkurawaranon, S. (2020). CT-Based measurements of facial parameters of healthy children and adolescents in Thailand. *American Journal of Neuroradiology*, 41(10), 1937-1942.

- Kannan, A., Sathyanarayana, H. P., & Padmanabhan, S. (2017). Effect of functional appliances on the airway dimensions in patients with skeletal class II malocclusion: A systematic review. *Journal of Orthodontic Science*, 6(2), 54.
- Kaur, M., Sharma, R. K., Tewari, S., & Narula, S. C. (2018). Influence of mouth breathing on outcome of scaling and root planing in chronic periodontitis. *BDJ open*, 4(1), 1-8.
- Kavand, G., Lagravère, M., Kula, K., Stewart, K., & Ghoneima, A. (2019). Retrospective CBCT analysis of airway volume changes after bone-borne vs tooth-borne rapid maxillary expansion. *The Angle Orthodontist*, 89(4), 566-574.
- KAZEMI DARABADI, S., AKBARI, G., Ebrahimi, E., & ZANGISHEH, M. (2018). Computed Tomographic Anatomy and Topography of the Lower Respiratory System of the Southern White-Breasted Hedgehog (*Erinaceus concolor*). *Iranian Journal of Veterinary Surgery*, 13(2 (29)), 589
- Kumar, S., Jayan, B., Kumar, M. P., Sharma, M., Nehra, K., & Bansal, A. K. (2019). Acoustic pharyngometry vs lateral cephalometry: A comparative evaluation of pharyngeal airway dimensions in patients with skeletal class I and skeletal class II malocclusion. *Orthodontic Waves*, 78(3), 118-125.
- Lagravère, M. O., Carey, J., Toogood, R. W., & Major, P. W. (2008). Three-dimensional accuracy of measurements made with software on cone-beam computed tomography images. *American Journal of Orthodontics Dentofacial Orthopedics*, 134(1), 112-116.
- Lee, C., Yoon, J., Han, S.-S., Na, J. Y., Lee, J.-H., Kim, Y. H., & Hwang, J. J. (2020). Dose assessment in dental cone-beam computed tomography: Comparison of optically stimulated luminescence dosimetry with Monte Carlo method. *PloS one*, 15(3), e0219103.

- Lee, K.-M., Davami, K., Hwang, H.-S., & Kang, B.-C. (2019). Effect of Voxel Size on the Accuracy of Landmark Identification in Cone-Beam Computed Tomography Images. *Journal of Korean Dental Science*, 12(1), 20-28.
- Li, B., Elango, J., & Wu, W. (2020). Recent Advancement of Molecular Structure and Biomaterial Function of Chitosan from Marine Organisms for Pharmaceutical and Nutraceutical Application. *Applied Sciences*, 10(14), 4719.
- Liao, Y.-F., & Lo, S. H. (2018). Surgical occlusion setup in correction of skeletal class III deformity using surgery-first approach: guidelines, characteristics and accuracy. *Scientific Reports*, 8(1), 1-8.
- Lohrabian, V., Kamali-Asl, A., Arabi, H., Mamashi, F., Hemmati, H. R., Zaidi, H., & Chemistry. (2019). Design and construction of a variable resolution cone-beam small animal mini-CT prototype for in vivo studies. *Radiation Physics*, 162, 199-207.
- Lorini, L., Ardighieri, L., Bozzola, A., Romani, C., Bignotti, E., Buglione, M., Tomasoni, M. (2021). Prognosis and management of recurrent and/or metastatic head and neck adenoid cystic carcinoma. *Oral oncology*, 115, 105213.
- Lun, Y., Lin, L., He, H., Ye, X., Zhu, Z., & Wei, Y. (2019). Effects of vortex structure on performance characteristics of a multiblade fan with inclined tongue. *Proceedings of the Institution of Mechanical Engineers*, 233(8), 1007-1021.
- Manhar, S., Shukla, C., Jain, U., Bharti, C., Shrivastava, T., & Dixit, S. (2019). Role of airway in orthodontic treatment planning-A Literature Review. *Journal Of Applied Dental Medical Sciences*, 5, 3.

- Maret, D., Telmon, N., Peters, O. A., Lepage, B., Treil, J., Inghèse, J., Sixou, M. (2012). Effect of voxel size on the accuracy of 3D reconstructions with cone beam CT. *Dentomaxillofacial Radiology*, 41(8), 649-655.
- Maurya, M. R. K., Kumar, C. P., Sharma, L. C. M., Nehra, L. C. K., Singh, H., & Chaudhari, P. K. (2019). Cephalometric appraisal of the effects of orthodontic treatment on total airway dimensions in adolescents. *J Oral Biol Craniofac Res*, 9(1), 51-56. doi:10.1016/j.jobcr.2018.09.004
- McGuigan, M. B., Duncan, H. F., & Horner, K. (2018). An analysis of effective dose optimization and its impact on image quality and diagnostic efficacy relating to dental cone beam computed tomography (CBCT). *Swiss dental journal*, 128(4), 297-316.
- McKeown, P., & Macaluso, M. (2017). Mouth Breathing: Physical, Mental and Emotional Consequences. Retrieved from <http://www.oralhealthgroup.com/features/mouth-breathing-physical-mental-emotional-consequences>
- Mete, A., & Akbudak, İ. (2018). Functional Anatomy and Physiology of Airway. In.
- Miller, L. E., Buzi, A., Williams, A., Rogers, R. S., Ortiz, A. G., Jones-Ho, K. O., & Elden, L. M. (2020). Reliability and accuracy of remote fiberoptic nasopharyngolaryngoscopy in the pediatric population. *Nose Throat Journal*, 0145561320919109.
- Mozzanica, F., Pizzorni, N., Scarponi, L., Crimi, G., & Schindler, A. (2020). Impact of Oral Myofunctional Therapy on Orofacial Myofunctional Status and Tongue Strength in Patients with Tongue Thrust. *Folia Phoniatica et Logopaedica*, 1-9.
- Mummolo, S., Nota, A., Caruso, S., Quinzi, V., Marchetti, E., & Marzo, G. (2018). Salivary markers and microbial flora in mouth breathing late adolescents. *BioMed research international*, 2018.

- Mutha, K. V. (2017). Effect of orthodontic treatment on the upper airway volume in adults. *Journal of Indian Orthodontic Society*, 51(3), 218-219.
- Pan, Y., Wang, X., Dai, F., Chen, G., & Xu, T. (2020). Accuracy and reliability of maxillary digital model (MDM) superimposition in evaluating teeth movement in adults compared with CBCT maxillary superimposition. *Scientific Reports*, 10(1), 1-8.
- Park, C.-A., & Kang, C.-K. (2017). Sensing the effects of mouth breathing by using 3-tesla MRI. *Journal of the Korean Physical Society*, 70(12), 1070-1076.
- Park, P., Kim, J., Song, Y. J., Lim, J. H., Cho, S. W., Won, T. B., Kim, H. J. (2017). Influencing factors on CPAP adherence and anatomic characteristics of upper airway in OSA subjects. *Medicine (Baltimore)*, 96(51), e8818. doi:10.1097/md.00000000000008818
- Patel, A. B. (2019). The impact of the presence of an anterior open bite on the oral health-related quality of life in adults. University of Birmingham,
- Pawłowska-Seredyńska, K., Umlawska, W., Resler, K., Morawska-Kochman, M., Pazdro-Zastawny, K., & Kręcicki, T. (2020). Craniofacial proportions in children with adenoid or adenotonsillar hypertrophy are related to disease duration and nasopharyngeal obstruction. *International journal of pediatric otorhinolaryngology*, 132, 109911.
- Pérez, W., Vazquez, N., & Ungerfeld, R. (2017). Gross Anatomy of Pampas Deer (*Ozotoceros bezoarticus*, Linnaeus 1758) Mouth and Pharynx. *Anatomia Histologia Embryologia*, 46(2), 195-203. doi:https://doi.org/10.1111/ahe.12257
- Purwanegara, M. K., Abdurachman, H., & Marsubrin, I. (2017). The development of a questionnaire, for early detection of upper respiratory tract obstruction, mouth breathing and adenoid face. *Journal of International Dental Medical Research*, 10, 628-636.

- Purwanegara, M. K., & Sutrisna, B. (2018). Mouth breathing, head posture, and prevalence of adenoid facies in patients with upper respiratory tract obstruction. *Journal of Dentistry Indonesia*, 25(1), 58-64.
- Quan, K., Tanno, R., Shipley, R. J., Brown, J. S., Jacob, J., Hurst, J. R., & Hawkes, D. J. (2019). Reproducibility of an airway tapering measurement in computed tomography with application to bronchiectasis. *Journal of Medical Imaging*, 6(3), 034003.
- Rasteau, S., Sigaux, N., Louvrier, A., & Bouletreau, P. (2020). Three-dimensional acquisition technologies for facial soft tissues—Applications and prospects in orthognathic surgery. *Journal of Stomatology, Oral Maxillofacial Surgery*, 121(6), 721-728.
- Recinto, C., Efthymeou, T., Boffelli, P. T., & Navalta, J. W. (2017). Effects of nasal or oral breathing on anaerobic power output and metabolic responses. *International Journal of Exercise Science*, 10(4), 506.
- Richmond, M. (2018). Evaluation of Craniofacial Superimposition as a Technique for Measuring Mountain Gorilla Facial Soft Tissue Depth and Implications for Hominid Facial Approximation. (Bachelors), The George Washington University.
- Rojas, E., Corvalán, R., Messen, E., & Sandoval, P. (2017). Upper airway assessment in Orthodontics: a review. *Odontoestomatologia*, 19(30).
- Saluja, K., Ravishankar, S., Ferrarotto, R., Zhu, H., Pytynia, K. B., & El-Naggar, A. K. (2020). Ectopic ACTH production and Cushing’s syndrome in a patient with parotid acinic cell carcinoma with high-grade transformation: tumor context and clinical implications. *Head and neck pathology*, 14(2), 562-569.
- San José, V., Bellot-Arcís, C., Tarazona, B., Zamora, N., Lagravère, M. O., & Paredes-Gallardo, V. (2017). Dental measurements and Bolton index reliability and accuracy

obtained from 2D digital, 3D segmented CBCT, and 3d intraoral laser scanner. *Journal of Clinical Experimental Dentistry*, 9(12), e1466.

- Shafiq-ul-Hassan, M., Zhang, G. G., Latifi, K., Ullah, G., Hunt, D. C., Balagurunathan, Y., Mackin, D. (2017). Intrinsic dependencies of CT radiomic features on voxel size and number of gray levels. *Medical physics*, 44(3), 1050-1062.
- Shaheen, E., Khalil, W., Ezeldeen, M., Van de Castele, E., Sun, Y., Politis, C., & Jacobs, R. (2017). Accuracy of segmentation of tooth structures using 3 different CBCT machines. *Oral Surgery, Oral Medicine, Oral Pathology Oral Radiology*, 123(1), 123-128.
- Shuhart, C. R., Yeap, S. S., Anderson, P. A., Jankowski, L. G., Lewiecki, E. M., Morse, L. R., Shepherd, J. A. (2019). Executive summary of the 2019 ISCD position development conference on monitoring treatment, DXA cross-calibration and least significant change, spinal cord injury, peri-prosthetic and orthopedic bone health, transgender medicine, and pediatrics. *Journal of Clinical Densitometry*, 22(4), 453-471.
- Sin, Ç., Akkaya, N., Aksoy, S., Orhan, K., & Öz, U. (2021). A deep learning algorithm proposal to automatic pharyngeal airway detection and segmentation on cbct images. *Orthodontics Craniofacial Research*.
- Smith, T., Ghoneima, A., Stewart, K., Liu, S., Eckert, G., Halum, S., & Kula, K. (2012). Three-dimensional computed tomography analysis of airway volume changes after rapid maxillary expansion. *Am J Orthod Dentofacial Orthop*, 141(5), 618-626. doi:10.1016/j.ajodo.2011.12.017
- Spin-Neto, R., Gotfredsen, E., & Wenzel, A. (2013). Impact of voxel size variation on CBCT-based diagnostic outcome in dentistry: a systematic review. *Journal of digital imaging*, 26(4), 813-820.

- Stratis, A., Zhang, G., Lopez-Rendon, X., Politis, C., Hermans, R., Jacobs, R., Bosmans, H. (2017). Two examples of indication specific radiation dose calculations in dental CBCT and Multidetector CT scanners. *Physica Medica*, 41, 71-77.
- Tanabe, N., Oguma, T., Sato, S., Kubo, T., Kozawa, S., Shima, H., Togashi, K. (2018). Quantitative measurement of airway dimensions using ultra-high resolution computed tomography. *Respiratory investigation*, 56(6), 489-496.
- Tayman, M. A., Kamburoğlu, K., Küçük, Ö., Ateş, F. S., & Günhan, M. (2019). Comparison of linear and volumetric measurements obtained from periodontal defects by using cone beam-CT and micro-CT: an in vitro study. *Clinical oral investigations*, 23(5), 2235-2244.
- Tzeng, Y. S., Hoffman, E., Cook-Granroth, J., Maurer, R., Shah, N., Mansour, J., Albert, M. (2007). Comparison of airway diameter measurements from an anthropomorphic airway tree phantom using hyperpolarized ³He MRI and high-resolution computed tomography. *Magnetic Resonance in Medicine*, 58(3), 636-642.
- Valcheva, Z., Arnautska, H., Dimova, M., Ivanova, G., & Atanasova, I. (2018). The role of mouth breathing on dentition development and formation. *Journal of IMAB—Annual Proceeding Scientific Papers*, 24(1), 1878-1882.
- Van Dessel, J., Nicolielo, L., Huang, Y., Coudyzer, W., Salmon, B., Lambrichts, I., & Jacobs, R. (2017). Accuracy and reliability of different cone beam computed tomography (CBCT) devices for structural analysis of alveolar bone in comparison with multislice CT and micro-CT. *European Journal of Oral Implantology*, 10(1), 95-105.
- van Egmond, M., Van Heerbeek, N., Ter Haar, E., & Rovers, M. (2017). Clinimetric properties of the Glasgow Health Status Inventory, Glasgow Benefit Inventory, Peak Nasal

Inspiratory Flow, and 4-Phase Rhinomanometry in adults with nasal obstruction. *Rhinology*, 55(2), 126-134.

- Wally, Y. R., Hussein, S. H., El-Karmouty, A. F., & Farid, M. F. (2020). Morphological studies and arterial supply of the pharynx in the goat (*Capra hircus*). *International Journal of Veterinary Science*, 9(2), 168-174. doi:10.37422/IJVS/20.008
- Whittier, D., Boyd, S., Burghardt, A., Paccou, J., Ghasem-Zadeh, A., Chapurlat, R., Bouxsein, M. (2020). Guidelines for the assessment of bone density and microarchitecture in vivo using high-resolution peripheral quantitative computed tomography. *Osteoporosis International*, 1-21.
- Wong, S.-M. S. (2019). Craniofacial signs, symptoms and orthodontic objectives of paediatric obstructive sleep apnoea. In L. E. (Ed.), *Sleep Disorders in Pediatric Dentistry* (pp. 57-87): Springer.
- Xiang, M., Hu, B., Liu, Y., Sun, J., & Song, J. (2017). Changes in airway dimensions following functional appliances in growing patients with skeletal class II malocclusion: A systematic review and meta-analysis. *International journal of pediatric otorhinolaryngology*, 97, 170-180.
- Yeh, J.-K., & Chen, C.-H. (2018). Estimated radiation risk of cancer from dental cone-beam computed tomography imaging in orthodontics patients. *BMC oral health*, 18(1), 1-8.
- Yılmaz, F., Kamburoğlu, K., & Şenel, B. (2017). Endodontic working length measurement using cone-beam computed tomographic images obtained at different voxel sizes and field of views, periapical radiography, and apex locator: a comparative ex vivo study. *Journal of endodontics*, 43(1), 152-156.

- Yilmaz, F., Sonmez, G., Kamburoglu, K., Koc, C., Ocak, M., & Celik, H. (2019). Accuracy of CBCT images in the volumetric assessment of residual root canal filling material: Effect of voxel size. *Nigerian journal of clinical practice*, 22(8), 1091.
- Yin, T., Jardine, M., Miles, A., & Allen, J. (2018). What is a normal pharynx? A videofluoroscopic study of anatomy in older adults. *Eur Arch Otorhinolaryngol*, 275(9), 2317-2323. doi:10.1007/s00405-018-5057-6
- Yu, H., Cho, S., Kim, M., Kim, W., Kim, J., & Choi, J. (2020). Automated skeletal classification with lateral cephalometry based on artificial intelligence. *J Dent Res*, 99(3), 249-256.
- Zhao, Y., Raco, J., Kourmatzis, A., Diasinos, S., Chan, H.-K., Yang, R., & Cheng, S. (2020). The effects of upper airway tissue motion on airflow dynamics. *Journal of Biomechanics*, 99, 109506.
- Zorba, E., Goutas, N., Spiliopoulou, C., & Moraitis, K. (2018). An evaluation of dental methods by Lamendin and Prince and Ubelaker for estimation of adult age in a sample of modern Greeks. *Homo*, 69(1-2), 17-28.